THESIS

UNTANGLING THE EFFECTS OF SEASONALITY AND POST-FIRE STREAM CHANNEL

EROSION ON THE HYDROLOGIC RESPONSE OF A BURNED MOUNTAIN CATCHMENT

Submitted by

Michael Gieschen

Department of Civil and Environmental Engineering

In partial fulfillment of the requirements

For the Degree of Master of Science

Colorado State University

Fort Collins, Colorado

Spring, 2022

Masters Committee:

     Advisor: Peter Nelson

     Tim Covino
     Pierre Julien

ABSTRACT

UNTANGLING THE EFFECTS OF SEASONALITY AND POST-FIRE STREAM CHANNEL

EROSION ON THE HYDROLOGIC RESPONSE OF A BURNED MOUNTAIN CATCHMENT

Stream channel incision and deposition are common after wildfire, and these geomorphic changes may impact runoff mechanisms and the composition of pre-event and event water in runoff. To investigate this, we monitored discharge and electrical conductivity at 6 nested sites within a 15.5 km^2 watershed in the northern Colorado Front Range that had recently burned, experienced large flooding, and well-documented and significant channel erosion and deposition. Over the study period, the watershed experienced seven precipitation events. For each hydrograph, we separate baseflow from runoff using a new method to characterize and account for the strong diurnal signal in the baseflow. Electrical conductivity is used as a tracer in a two-component end-member mixing analysis to separate the event hydrographs into event and pre-event water. Correlation coefficients were computed between key variables of the hydrologic response (such as runoff ratio, volumes of event and pre-event water) to storm and basin characteristics (including stream channel erosion/deposition, fraction of high/moderate burn severity, precipitation intensity, and antecedent precipitation). The strength and significance of correlations was found to vary seasonally. In the early season, event and pre-event volumes did not vary significantly with basin or storm characteristics. In the late season, antecedent precipitation correlated with a decrease in event runoff ($R^2 = 0.34$) and total runoff ($R^2 = 0.40$), increased precipitation intensity correlated with an increase in event runoff ($R^2 = 0.48$), and local erosion correlated with an increase in pre-event runoff ($R^2 = 0.60$) and total runoff ($R^2 = 0.53$). These findings indicate that seasonality and post-fire stream channel erosion influence the makeup of runoff response, most likely through their impact on the gradient of the near-stream groundwater table.

TABLE OF CONTENTS

INTRODUCTION

Wildfires impact a wide range of ecological, hydrologic, and geomorphic processes. Studies investigating the effects of wildfires on hydrologic response and event runoff have shown that fire and soil heating can affect the infiltration and hydraulic connectivity of soils by creating hydrophobic soils, (Ebel, 2012; Ebel and Moody, 2013; Ebel 2019) or soil sealing (Larsen et al., 2009). Infiltration rates and porosity can also be affected (Imeson et al. 1992), both of which can impact whether runoff during and after storms is composed of event water or pre-event water. Furthermore, destruction of vegetation by wildfire has been found to increase runoff ratios (Stoof et al, 2012). Vegetation removal by fire to the effects of vegetation removal by clear cutting and found that the increased water repellency of soil following the wildfire had the greater effect on generation of event water during storm runoff (Scott, 1997). Work on wildfires in Mongolia (Kopp, 2017) has shown that increased soil water repellency following a wildfire can interact with other geologic and topographic conditions of the basin, such as a seasonally melting permafrost, to alter the expected hydrologic runoff response.

The effects of wildfire go beyond the immediate impacts of hydrophobic soils and burned vegetation, however. Geomorphic processes such as sediment delivery to channels, hillslope erosion, and erosion and deposition within the channel network have been shown to accelerate after wildfire, especially when the fire is followed quickly by significant runoff events (Kampf et al, 2016; Brogan et al, 2017, 2019a, 2019b). These post-fire changes can compound the fire's effects on basin hydrology and have been shown to affect the timing of damaging debris flows (McGuire and Youberg, 2019; Raymond et al., 2020). However, it is not clear how these geomorphic changes may affect watershed hydrologic response.

The relative contribution of event and pre-event water in runoff is impacted by watershed characteristics such as the degree of urbanization (Pellerin et al, 2008) and deforestation (Scott, 1997). Studies on forested mountain catchments have found some consistency in response to some storm and basin characteristics and event/pre-event water compositions using various approaches for hydrograph

1

separation, including isotopes and electrical conductivity (Klaus and McDonnell, 2013). In particular, event and pre-event water have been found to be correlated with precipitation intensity (Blume et al 2007; Noriato et al 2009; McDonnell, 1990; Matsubayashi, 1993) and the boundary state of soil wetness, or antecedent precipitation (von Freyberg et al., 2018; Litt et al., 2015; Sidle et al, 2015; Inamdar et al., 2013; Brown et al., 1999). However, the effects of post-fire geomorphic changes on the event/pre-event water composition have not been investigated.

Electrical conductivity (EC) is especially useful for studying the hydrologic response in systems with high-intensity, short-duration storms, due to ability to collect measurements with a high temporal resolution. The use of EC as a method of hydrograph separation has been used for decades (Pilgrim et al, 1979) and has become more popular due to the low cost and ease of installation, particularly in alpine and other difficult to access locations (Cano-Paolini et al, 2019; Engel et al., 2018; Laudon and Slaymaker, 1997). While EC is a non-conservative tracer compared to other methods of hydrograph separation such as measuring stable isotopes, some studies have shown that EC can produce comparable results and can be used as a reliable method of separating event water from pre-event water, especially when precipitation and groundwater have significantly different EC signatures (Lott and Stewart, 2016; Matsubayashi et al., 1993; Pellerin et al., 2008; Klaus and McDonnell, 2013).

Here we investigate the characteristics of hydrologic response of a mountain catchment that experienced moderate to severe wildfire three years prior to the study and a major geomorphically effective flood two years prior to the study (Brogan et al., 2017). We use field measurements of precipitation, stream depth and electrical conductivity distributed throughout the catchment to characterize runoff response during and after summer storms. We develop event hydrographs from stream depth measurements for the period of the study and use EC as a tracer in a mass balance equation to separate the hydrographs into event water and pre-event water.

We use our observations to address the following questions:

1. Is the composition of storm-event runoff affected by burn severity, recent channel erosion/deposition, or other wildfire/geomorphic response characteristics?

2

2. What are the storm characteristics that affect the composition of runoff in a disturbed mountain catchment and what underlying mechanisms could explain this response?

And through our investigation a follow-up question became necessary:

3. Is event runoff composition affected by water table gradients which vary with local erosion and the season in which the event occurs?
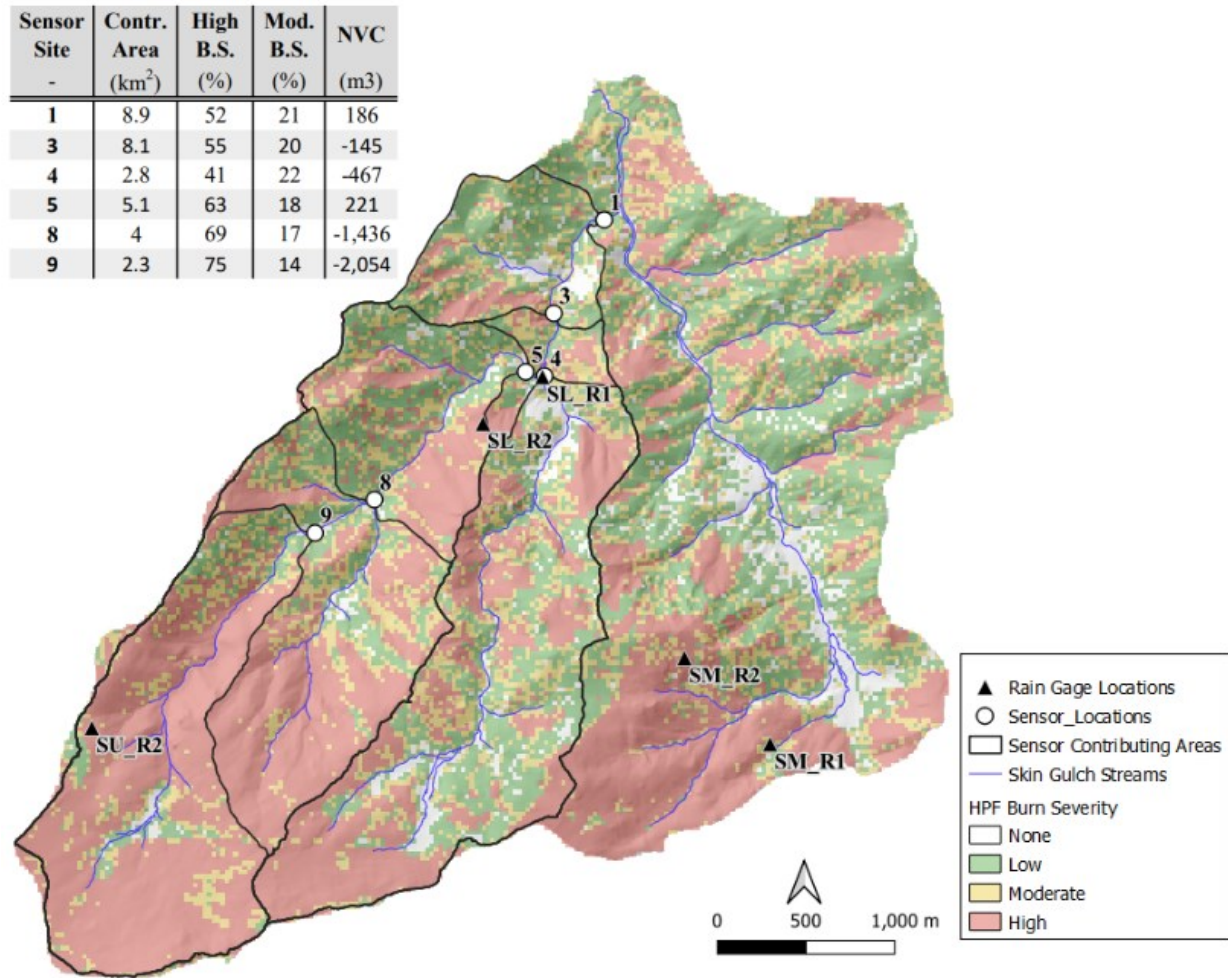
METHODS

Study Area

Skin Gulch is a 15.5 km^2 tributary basin to the Cache la Poudre River in north central Colorado with two primary branches (Figure 1). This study focuses on the western branch which is 8.9 km^2 in area and occupies elevations ranging from 1890 m to 2580 m. The precipitation patterns in the basin are typically characterized by snowfall from November to May, and short, high-intensity convective storms through the summer months. Underlying geology in the basin consists of primarily Precambrian metamorphic schists, gneiss, and igneous rocks with Redfeather sandy loam soils (Abbott, 1970). The basin lies on the Stove Prairie Fault line and the western branch that this study focuses on coincides with a shear zone, which other studies have shown may influence flow locations and channel head initiation (Martin et al., 2021).

In 2012 the High Park wildfire burned more than 350 km^2 in the Colorado Front Range, including the Skin Gulch watershed. Over 50% of the Skin Gulch study area was classified as high burn severity, with an additional 20% classified as moderate burn severity (Figure 1). Several rainfall events following the fire caused significant changes to the landscape and geomorphic processes in the in basin. The convective storms in the months following the fire caused large amounts of hillslope material transport and deposition in the lower reaches of the watershed (Kampf et al. 2016, Brogan et al. 2017).

In September 2013, one year after the fire, a high-volume, long-duration storm caused widespread flooding and damage to the area of the Colorado Front Range. This flood had significant geomorphic impacts on the Skin Gulch watershed, flushing sediment and causing significant erosion through many sections of the channel (Brogan et al. 2017, 2019). Differencing of repeat airborne LiDAR digital elevation models collected over a 4-year period following the fire and storms found that sediment volume changes in the stream corridor were correlated with contributing area, channel width, and percent high or moderate burn severity, among other factors (Brogan et al, 2019b). Data from that analysis are used in the present paper to characterize geomorphic variables for the site.

4

Sensor Site	Contr. Area (km^2)	High B.S. (%)	Mod. B.S. (%)	NVC (m3)
1	8.9	52	21	186
3	8.1	55	20	-145
4	2.8	41	22	-467
5	5.1	63	18	221
8	4	69	17	-1,436
9	2.3	75	14	-2,054

Figure 1. Skin Gulch basin area overlain with burn severity levels. Rain gage sensors are labeled SU (upper elevations) SM (for middle elevations) and SL (for lower elevations). CTD-10 sensor sites are labeled 1,3,4,5,8, and 9. The inset table shows contributing area, burn severity percentages, and erosion (NVC) data for each site (NVC < 0 corresponds to net erosion, NVC > 0 corresponds to net deposition).

Discharge and EC Measurements

Decagon CTD-10 sensors were placed at 6 locations within the Skin Gulch watershed, as shown in Figure 1. The CTD sensor employs a vented pressure transducer, a 4-probe electrical conductivity transducer, and a thermistor to measure depth, EC, and temperature, respectively. Water depth is automatically corrected for changes in barometric pressure through venting. EC is automatically temperature corrected based on the procedure outlined in the US Salinity Labs Handbook 60 (USDA Labratory Staff, 1954).

Depth and EC were measured continuously at each sensor location in 1-minute increments from June through October 2015. Because the CTD-10 sensor cannot operate in freezing conditions, measurements were taken throughout the freeze-free period only.

Depth-discharge rating curves were developed for each sensor location based on 7 manual discharge measurements made at each site throughout the season. In the early season when flow depths were adequate, a Sontek Stream Tracker acoustic doppler velocimeter was used to measure stream velocity along a cross section. Velocity and depth measurements were taken at 0.1 m increments across the stream, and the velocity-cross sectional area method was used to develop a discharge rating for each site. In the latter part of the season, when shallow depths made the use of the velocimeter difficult, discharge was measured using a slug injection method (Day, 1976; Moore, 2005). Recent studies have shown this is a comparable substitute for traditional stream gaging methods (Weijs et al, 2013). Per methodology outlined in the literature (Hudson and Fraser, 2005), a salt solution with 2 kg per 1 m^3/s of discharge was added to the stream. For Skin Gulch this equated to 1-L solutions of table salt at 100 g/L applied at each slug injection. This solution was injected 50 meters (approximately 25 stream widths) upstream of each sensor. During the slug injections, the CTD-10 sensors were set to measure depth and EC every 10 seconds and changed back to 1-minute intervals after the slug injection was completed. These measurements did not coincide with any of the storms measured in this analysis and no impact to the EC was noted after the slug injection. Due to the recession of baseflow throughout the season, measurements during high baseflow conditions at the beginning of the season were higher than almost all of the individual storm-event discharges.

Storm Identification, Baseflow Separation, and Removal of Diurnal Fluctuations

Seven discharge events were registered by the sensors and were isolated for analysis. A total of 34 hydrographs were developed from 6 sites and 7 storms, with 8 site/storm combinations being excluded due to sensor malfunction or stream discharge dropping below the depth of the sensor.

Outside of these events, baseflow stream discharge receded throughout the season to between 20-30% of the baseflow discharge at the time of the first event in June (Figure 2). It should be noted that the

1 July storm (Storm 4) produced discharge volumes high enough to significantly influence the baseflow recession trend. At all sensor sites, baseflow discharge exhibited significant diurnal fluctuations throughout the season, shown in Figure 2.

In order determine the seasonal trend of baseflow a line was fitted to the discharge record at the minimum flow value for each day in the segments of the hydrograph outside of the identified storm events, which is a method that has been used by other studies. This line was used as the baseflow trend for the entire season. However, when separating the baseflow from an individual storm event this trendline underpredicted the baseflow due to significant diurnal fluctuations.

Therefore, we developed a new method to account for the diurnal fluctuations in the baseflow. A more detailed line that captures the daily variation in discharge was fitted to the segments of the hydrograph between storm events using a Bayesian spline fit procedure (D'Errico, 2021); one of these sections is shown in detail in Figure 2c. This line was used to calculate the difference between the diurnal fluctuations and the seasonal baseflow trend. This variation was normalized to the time of day and an average daily time series of variations, shown in Figure 2d, was calculated for each recession segment of the hydrograph. These averages were added to the baseflow trends during the individual storm events to create a more accurate representation of the baseflow during that event.

EC may also have exhibited similar diurnal fluctuations during the non-storm recession periods. However, the magnitude of these fluctuations did not exceed the normal variability in the data, and therefore baseflow EC for each storm event was assumed to be a constant equal to the average EC for the 3 hours preceding each storm event.
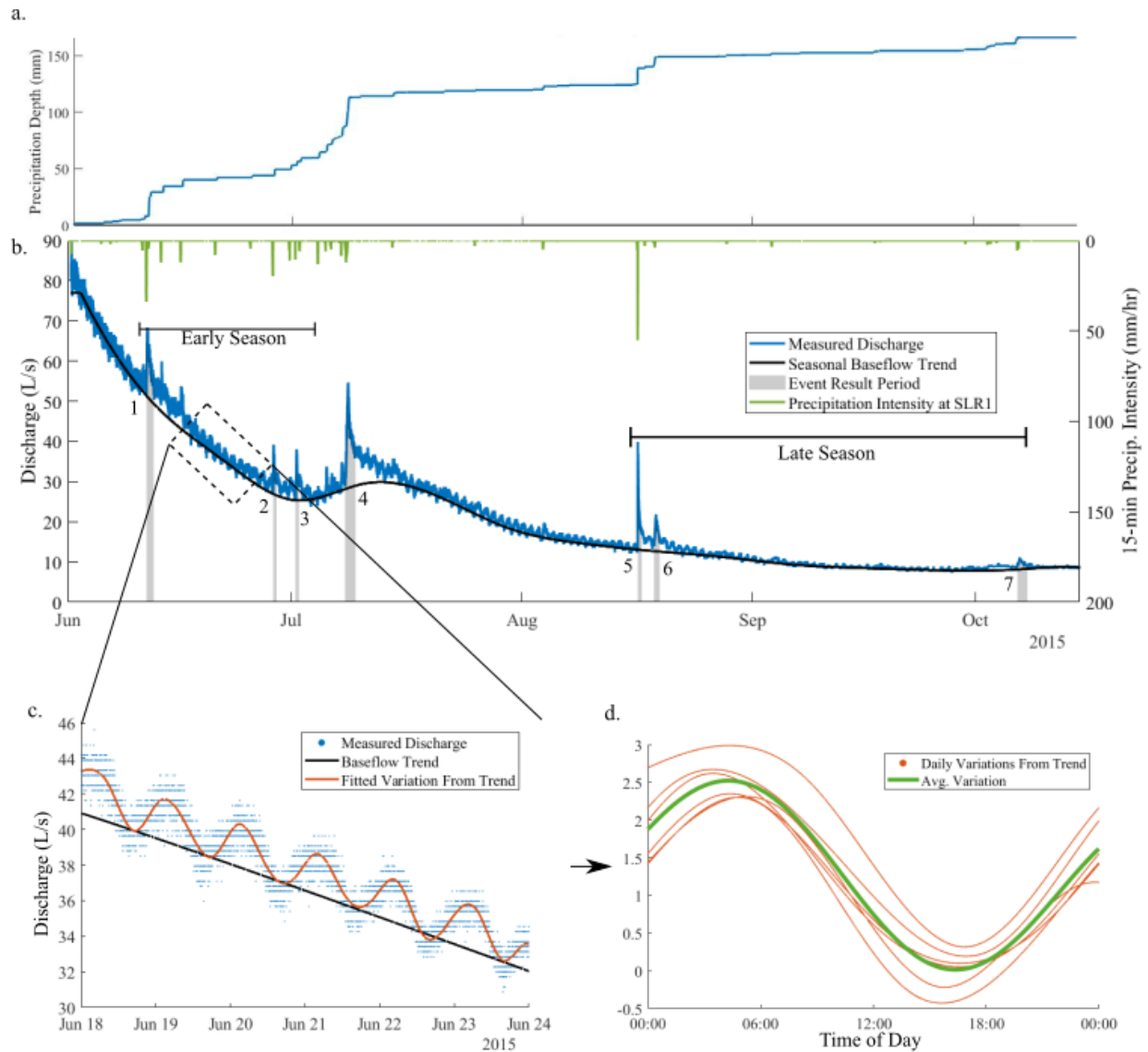
Figure 2. *a) Cumulative precipitation depth for rain gage SLR1. b) Discharge record for Site 3 from June to October 2015. Duration of the identified storm events is shown in grey with their corresponding storm number. Storms 1, 2, and 3 were considered early season, and Storms 4, 5, and 6, were considered late season. The fitted seasonal baseflow trend is shown as the black line. c) The diurnal variation from the baseflow trend in a segment of the hydrograph between storm events with the line that was fitted to the data account for that variation. d) Daily time series of the diurnal variation and the average of those series, which is applied as the baseflow adjustment in Figure 4.*

Hydrograph Separation

Individual storm events were extracted from the overall time series of discharge (Figure 2a) and

EC for each site, and lines were fit to both the EC and discharge during each event to filter out

measurement variability (Figure 3) using the Bayesian spline fit procedure (D'Errico, 2021). Storm event

durations were trimmed to the time when the storm event discharge (total discharge minus baseflow) reached 10% of the peak storm discharge (Figure 4).
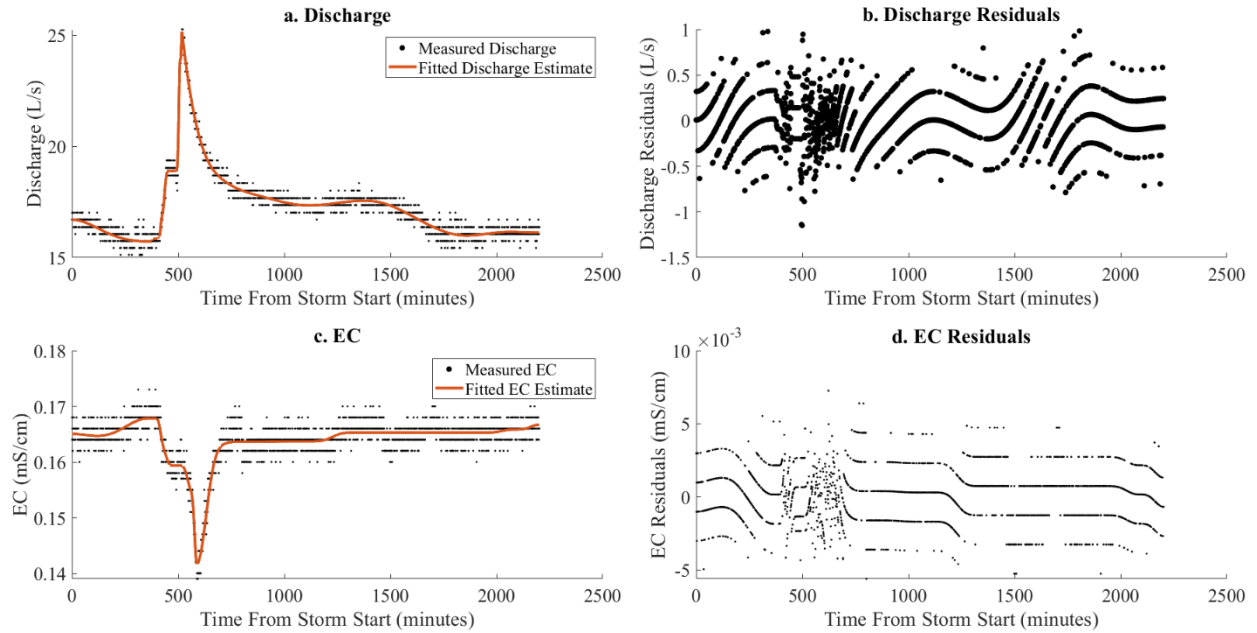
Figure 3. *Discharge (a) and EC (c) measurements for Site 8 Storm 3 along with the fitted lines used for calculations. (b) and (d) show the residuals for Discharge and EC respectively.*

Hydrograph separation was performed using the two-component mass balance equations below to calculate event and pre-event runoff:

$$q_t = q_{bf} + q_{pe} + q_e \tag{1}$$

$$q_t C_t = q_{bf} C_{bf} + q_{pe} C_{pe} + q_e C_e \tag{2}$$

where q is the instantaneous discharge at each timestep and C is the instantaneous EC level at each timestep during the storm event. The subscripts refer to: total discharge (t) baseflow (bf), pre-event water (pe), and event water (e). This procedure has been outlined in multiple studies (Kronholm and Capel, 2015; Lott and Stewart, 2016; Pellerin et al, 2007) and several assumptions about the EC of end members are necessary for this analysis. Event water was assumed to have similar EC as the precipitation, as has been used in other studies (Pellerin, 2007; Buttle et al., 1995. The National Atmospheric Deposition Program (NADP, 2021) collects weekly data of various water quality metrics of precipitation, including EC, at sites throughout the country. Electrical conductivity for precipitation and event water was based on

the weekly data from NADP site CO19 located in Rocky Mountain National Park, 37 km southwest of

our project site. These data were compared to other nearby NADP sensors to check for similarity during

the storm events to ensure no outlier data were being used. All precipitation EC values during storm

events range from 0.005 mS/cm to 0.017 mS/cm, which are an order of magnitude less than EC values

observed in Skin Gulch during baseflow periods. Precipitation EC differing significantly from

background or baseflow is a necessary assumption of using EC as a tracer for event/pre-event water

(Kronholm and Capel, 2015; Pellerin, 2007).
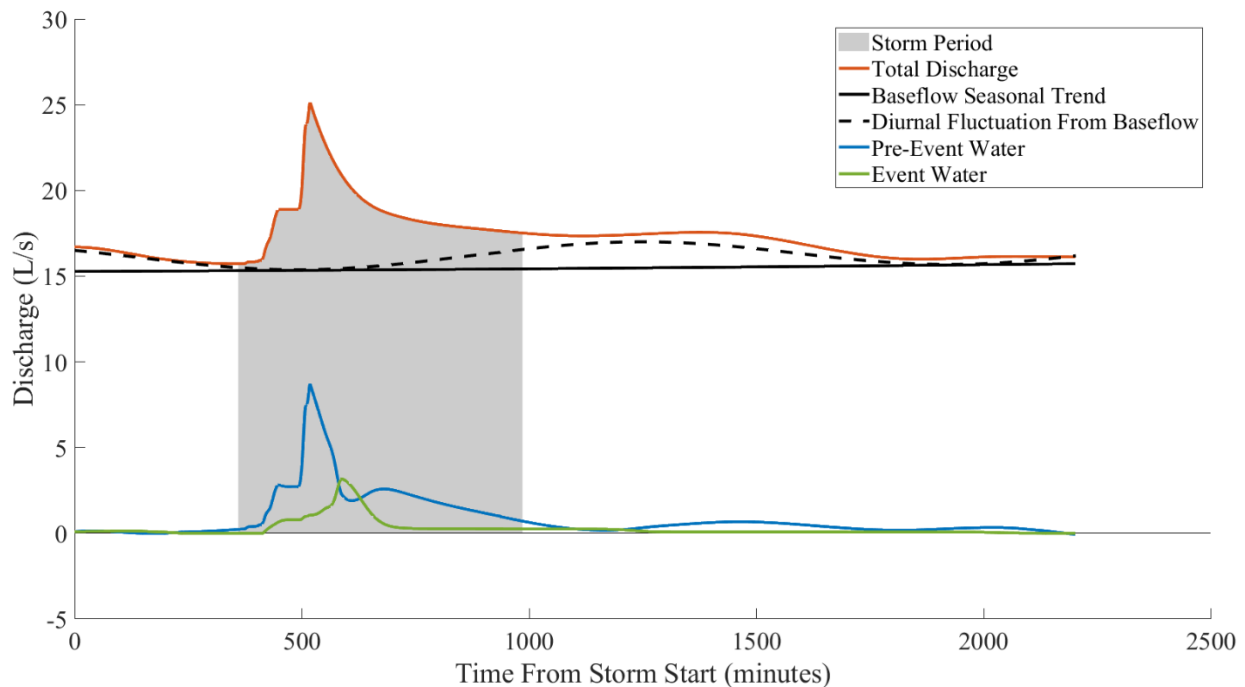
Figure 4: *Hydrograph Separation of Site 8 Storm 3. The solid black line represents the seasonal baseflow trend. The dashed black line shows the adjustment made to the baseflow based on the diurnal fluctuations of the preceding recession period. The red line shows the total discharge, and the blue and green lines show the calculated pre-event and event water discharges respectively. The gray area shows the storm period over which event results were calculated.*

Baseflow and pre-event EC (C_{bf}, C_{pe}) were assumed to be equal to the average EC observed

during the 3 hours before any increase in discharge (values range from 0.11 mS/cm to 0.19 mS/cm).

Additionally, the discharge of the baseflow throughout the storm was calculated based on the baseflow

separation methods described above. Therefore, Q_{bf} and C_{bf} are known variables in equations 1 and 2.

With these assumptions Q_e and Q_{pe} can be solved for using equations 1 and 2. Figure 4 shows an example

of the resulting event hydrograph separation. Based on these hydrograph separations the hydrologic variables shown in Table 2 were calculated.

Precipitation Data

Precipitation data were collected at the 5 sites shown in Figure 1, using RainWise tipping bucket rain gages. Peak 15-minute rainfall intensity and cumulative depth of rainfall were calculated for each of the rain gage sites. Grided rasters of these data were created using inverse distance weighting (IDW) between the rain gages and across the study area. These rasters were used to calculate a spatial average of the 15-minute intensities for each storm within the contributing area of each of the depth/EC sensor sites and to calculate the total storm volume of precipitation (P) from cumulative depth across the contributing area of each depth/EC sensor site. The same method of IDW raster generation was also used to calculate precipitation volumes for the 5 and 10 days prior to each storm.

Geomorphic Data

Previous studies on Skin Gulch (Brogan et al., 2019b) used analysis of repeat airborne LiDAR data sets and raster differencing to calculate geomorphic and topographic information in 50-m segments of the stream. For this study, geomorphic and topographic variables of net volume change, percent area of high and moderate burn severity, and contributing area, described for each site in Figure 1, were examined from the time period of 2012, just after the High Park Fire but before the large flood in 2013, to the beginning of 2015 when this hydrologic information was collected. The geomorphic variables used for this study were combined from the segment that contained the depth/EC sensor and the segments immediately upstream and downstream of that segment, for total reach length of 150 m around each sensor site.

Analysis

Ordinary least squares linear regression was used to compare key variables of the hydrologic response (runoff ratio (RR), volume of event water per precipitation (V_e/P), volume of pre-event water per precipitation (V_{pe}/P), volume of pre-event water per volume of storm discharge (V_{pe}/V_{st}), peak event water discharge per peak total discharge (Q_e/Q_t), peak pre-event water per peak total discharge (Q_{pe}/Q_t)) to

storm and basin characteristics (net volume change of sediment in the stream corridor (*NVC)*, fraction of contributing area with moderate burn severity (*Mod. B.S.*), fraction of contributing area with high burn severity (High B.S.), 15-minute precipitation intensity (I_{15}), volume of precipitation in the 10 days preceding the storm event (AP_{10}), volume of precipitation in the 10 days preceding the storm event (AP_5), and volume of precipitation for the storm event (*P*)) shown in Table 1. Volumetric hydrologic response variables have been normalized by the precipitation volume of the associated storm (*RR*, V_e/P, V_{pe}/P). This method of examining hydrologic response variables has been advocated for in other studies (von Freyberg et al., 2018; Blume et al. 2007) and helps account for both basin size and storm size when considering hydrologic response. Similarly, peak discharge of event water and pre-event water, have been normalized by the peak total discharge of the storm in which they occur (Q_e/Q_t, Q_{pe}/Q_t) to allow comparison of event and pre-event water peaks between storms. Correlation *p*-values (*p*) were calculated for each comparison to account for varying number of data points and correlations with $p < 0.05$ considered significant for this analysis.

Table 1. *Acronyms and definitions for variables used in the analysis of results.*

Acronym	Variable	Definition
Basin Characteristics		
NVC	Net Volume Change	Change of sediment volume in the stream corridor. Positive is deposition, negative is erosion.
Mod. B.S.	Moderate Burn Severity	Percent of contributing area that was burned with moderate intensity.
High B.S.	High Burn Severity	Percent of contributing area that was burned with high intensity.
Precipitation Characteristics		
AP_{10}	10-Day Antecedent Precipitation	Volume of Precipitation occurring in the 10 days before the storm event.
AP_5	5-Day Antecedent Precipitation	Volume of Precipitation occurring in the 5 days before the storm event.
I_{15}	15-Min. Storm Intensity	Peak 15-minute intensity of event precipitation.
P	Precipitation Volume	Volume of precipitation, expressed in depth per contributing area.
Runoff Characteristics		
V_t	Volume of Total Discharge	Total volume of the discharge that occurs during the event.
V_{st}	Volume of Storm Runoff	Volume of runoff: Total discharge volume, minus volume of baseflow during the event.
V_e	Volume of Event Water Runoff	Volumetric portion of the storm runoff that has an EC signature similar to precipitation.
V_{pe}	Volume of Pre-Event Water Runoff	Volumetric portion of the storm runoff that has an EC signature similar to the baseflow.
Q_t	Peak Total Discharge	Peak flow of total discharge that occurs during the event.
Q_{bf}	Baseflow Discharge	Average discharge of baseflow just before the event.
Q_e	Peak Event Discharge	Instantaneous discharge peak of the event water runoff.
Q_{pe}	Peak Pre-Event Discharge	Instantaneous discharge peak of the pre-event water runoff.
Analysis Variables		
V_e/P	Volume of Event Runoff Per Precipitation	Volume of event water divided by the precipitation volume.
V_{pe}/P	Volume of Pre-Event Runoff Per Precipitation	Volume of pre-event water divided by the precipitation volume.
RR	Runoff Ratio	Volume of Event Discharge per precipitation volume (V_{st}/P). Note: $RR = V_e/P + V_{pe}/P$.
Q_e/Q_t	Peak Event Discharge per Peak Total Discharge	Event discharge normalized to total discharge for comparison.
Q_{pe}/Q_t	Peak Pre-Event Discharge per Peak Total Discharge	Pre-event discharge normalized to total discharge for comparison

13

RESULTS

Precipitation

Table 2 provides an overview of the precipitation data for each site and storm. Total storm precipitation volumes ranged from 12 to 209 mm-km^2 and peak 15-min precipitation intensities ranged from 4.5 to 36.3 mm/hr. Storm 5 on 16 August produced the highest intensity rainfall event for all sites (17.5 to 30.2 mm/hr), but due to having a shorter duration it only produced between 12 and 63 mm-km^2 of cumulative volume. In contrast, Storm 4 on 8 July only had moderate precipitation intensities (9.9 to 11.5 mm/hr) but with storm durations lasting more than 10 hours and significant preceding precipitation, produced the highest cumulative volume at all of the site locations (51 to 209 mm-km^2). These two storms were the most significant of the summer and have been noted in other work in Skin Gulch (Wilson et al., 2021) as producing the highest amount of hillslope erosion and sediment movement for this season.

Hydrologic Response

Total storm discharge volumes (V_{st}) ranged from 60 m^3 to 3971 m^3 and the fraction of discharge that was pre-event water (V_{pe}/V_{st}) ranged from 0.3 to 0.99. Total discharge peaks (Q_t) ranged from 9.5 L/s to 91.7 L/s and the pre-event peaks per total peak (Q_{pe}/Q_t) ranged from 12% to 58%. Runoff ratios (*RR*, volume of storm discharge per volume of precipitation) ranged from 0.2% to 2% over the study period. Volume of pre-event water per precipitation (V_{pe}/P) ranged from 0.04% to 1.6% and volume of event water per precipitation (V_e/P) ranged from 0.03% to 0.8%.

Correlations with Hydrologic Response

Correlations between hydrologic response volumes and peak discharges were compared to the basin and storm characteristics shown in Table 3. Results were separated into early season (Storms 1, 2, and 3) and late season (Storms 5, 6, and 7) shown in Figure 2. Storm 4 was excluded from this data segregation as it occurred at the transition of high and low baseflow and had a noted effect on the overall

Table 2. *Results of the hydrologic response analysis: Average Baseflow (Q_{bf}), Peak Total Discharge (Q_t), Peak Event and Pre-Event Flow per Peak Total Flow (Q_e/Q_t and Q_{pe}/Q_t), Total Volume of Discharge (V_t), Volume of Storm Discharge or Total Discharge Minus Baseflow (V_{st}), Volume of Event and Pre-Event Discharge (V_e and V_{pe}), Ratio of Event and Pre-Event Discharge to Storm Discharge (V_e/V_{st} and V_{pe}/V_{st}); results of the precipitation analysis: Volume of precipitation (P), Volume of 5 Day Antecedent Precipitation (AP_5), Volume of 10 Day Antecedent Precipitation (AP_{10}), 15-Minute Precipitation Intensity (I_{15}); and hydrologic response results in terms of precipitation: Runoff Ratio or Volume of Storm Discharge per Precipitation Volume (RR), Volume of Event and Pre-Event Water per Precipitation Volume (V_e/P and V_{pe}/P)*

Storm	Site	Hydrologic Response										Precipitation				Response Per Precip.		
		Q_{bf}	Q_t	Q_e/Q_t	Q_{pe}/Q_t	V_t	V_{st}	V_e	V_{pe}	V_e/V_{st}	V_{pe}/V_{st}	P	AP_5	AP_{10}	I_{15}	RR	V_e/P	V_{pe}/P
-	-	(L/s)	(L/s)	-	-	(m^3)	(m^3)	(m^3)	(m^3)	-	-	(mm-km^2)	(mm-km^2)	(mm-km^2)	(mm/hr)	-	-	-
11-June Storm 1	1	67.4	91.7	8%	23%	6,928	1,152	278	875	24%	76%	116	47	59	18.1	0.99%	0.24%	0.75%
	3	54.5	66.6	7%	13%	5,043	543	181	361	33%	67%	105	43	54	17.2	0.52%	0.17%	0.35%
	4	21.5	25.6	7%	12%	1,908	183	51	132	28%	72%	35	14	17	17.7	0.52%	0.14%	0.37%
	5	34.4	42.4	11%	12%	2,063	263	179	84	68%	32%	65	28	36	16.3	0.40%	0.27%	0.13%
	8	27.1	34.2	9%	16%	2,547	259	58	201	22%	78%	51	22	29	14.5	0.51%	0.12%	0.40%
	9	33.3	45.3	8%	20%	2,682	321	95	226	30%	70%	28	13	17	12.4	1.14%	0.34%	0.80%
28-June Storm 2	1	35.3	58.2	7%	43%	1,964	694	91	603	0.1	87%	56	37	43	19.3	1.25%	0.16%	1.09%
	3	28.8	38.4	9%	20%	1,328	217	78	139	0.4	64%	51	36	40	19.1	0.43%	0.15%	0.27%
	5	22.9	27.5	6%	16%	1,017	114	55	59	0.5	52%	33	27	30	19.4	0.35%	0.17%	0.18%
	8	16.6	21.7	10%	19%	802	100	21	79	0.2	79%	25	25	27	18.3	0.39%	0.08%	0.31%
	9	18.0	24.5	9%	20%	1,125	130	27	104	0.2	80%	14	18	19	17.4	0.92%	0.19%	0.73%
1-July Storm 3	1	32.6	54.6	3%	43%	1,865	521	45	476	9%	91%	58	91	128	21.4	0.90%	0.08%	0.82%
	3	27.1	37.7	5%	28%	1,272	187	49	138	26%	74%	55	83	119	22.4	0.34%	0.09%	0.25%
	5	21.9	29.2	5%	25%	907	124	45	79	36%	64%	39	54	82	25.9	0.32%	0.11%	0.20%
	8	16.0	25.1	13%	35%	704	113	27	87	23%	77%	35	43	68	30.2	0.32%	0.08%	0.25%
	9	16.8	39.9	20%	52%	724	194	60	134	31%	69%	24	25	43	36.3	0.82%	0.26%	0.57%
8-July Storm 4	1	42.4	90.2	14%	52%	8,444	3,971	646	3324	0.2	84%	209	259	431	11.0	1.90%	0.31%	1.59%
	3	29.8	52.7	14%	33%	5,093	1,513	358	1156	0.2	76%	190	237	397	10.9	0.80%	0.19%	0.61%
	5	22.0	33.5	17%	20%	3,502	673	440	233	0.7	35%	119	150	257	10.6	0.57%	0.37%	0.20%
	8	17.1	28.5	15%	28%	2,579	610	165	445	0.3	73%	91	119	208	10.3	0.67%	0.18%	0.49%
	9	17.2	37.9	15%	41%	3,001	952	216	737	0.2	77%	51	68	122	9.9	1.87%	0.42%	1.44%
16-Aug. Storm 5	3	13.3	39.0	24%	45%	1,032	438	83	355	19%	81%	63	16	17	28.4	0.69%	0.13%	0.56%
	4	9.1	34.1	33%	47%	349	123	85	37	70%	30%	23	4	5	29.8	0.54%	0.38%	0.17%
	5	13.5	39.1	27%	40%	454	131	55	77	42%	58%	37	11	12	26.4	0.35%	0.15%	0.20%
	8	9.8	17.0	13%	35%	566	132	20	112	15%	85%	24	10	10	21.4	0.54%	0.08%	0.46%
	9	8.7	15.0	14%	29%	451	99	15	84	15%	85%	12	7	7	17.5	0.85%	0.13%	0.72%
18-Aug. Storm 6	3	14.2	21.2	5%	26%	1,198	214	22	192	0.1	90%	74	84	91	4.6	0.29%	0.03%	0.26%
	4	9.7	12.2	6%	14%	944	87	22	64	0.3	74%	26	29	31	4.5	0.34%	0.09%	0.25%
	5	13.7	37.3	5%	58%	504	109	18	92	0.2	84%	46	51	57	4.8	0.24%	0.04%	0.20%
	8	10.5	14.6	6%	23%	1,234	147	15	132	0.1	90%	37	36	41	5.0	0.40%	0.04%	0.36%
	9	9.4	14.7	4%	31%	897	131	28	104	0.2	79%	21	19	22	5.1	0.63%	0.13%	0.50%
6-Oct. Storm 7	3	8.8	10.6	0%	16%	1,124	106	1	104	1%	99%	48	27	43	6.0	0.22%	0.003%	0.22%
	4	8.0	9.5	3%	16%	614	60	13	47	21%	79%	14	6	11	5.3	0.42%	0.09%	0.33%
	9	6.6	9.6	4%	29%	854	115	14	101	12%	88%	16	9	15	7.6	0.73%	0.09%	0.65%

baseflow for several weeks after the event. The entire period of record included 34 hydrographs, the early season included 16 hydrographs and the late season 13 hydrographs.

During the entire period of record, pre-event water per precipitation (V_{pe}/P) was highly correlated with runoff ratio (RR) ($R^2 = 0.94$). Event water per precipitation (V_e/P) also had a significant correlation with the overall runoff ratio ($R^2 = 0.39$), but with a much weaker signal. The ratio of peak event water to total peak discharge (Q_e/Q_t) was moderately correlated with peak 15-minute storm intensity ($R^2 = 0.32$). During the early season, volume of antecedent precipitation (AP_5 and AP_{10}) had no significant correlation with the overall volumes of runoff (RR), event water (V_e/P) and pre-event water (V_{pe}/P). In the late season however, antecedent precipitation (AP_{10}) was negatively correlated with volume of event water per precipitation (V_e/P) ($R^2 = 0.34$), but did not have a significant correlation with the volume of pre-event water (V_{pe}/P). Antecedent precipitation (AP_{10}) also correlated (negatively) with total runoff volume per precipitation (RR) ($R^2 = 0.41$), indicating that preceding precipitation led to a decrease in the overall amount of runoff from precipitation as well as a decrease in the event water per precipitation.

Likewise for 15-minute precipitation intensity (I_{15}), storms with higher intensity in the early season correlated with only the relative peaks of both event water (Q_e/Q_t) and pre-event water (Q_{pe}/Q_t) ($R^2 = 0.31$ and 0.53), both increasing with greater precipitation intensity. However, overall volumes of event water (V_e/P) and pre-event water (V_{pe}/P) did not increase with greater storm intensity in the early season. In the late season, precipitation intensity (I_{15}) was very highly correlated ($R^2 = 0.91$) with an increase in relative peak of the event water (Q_e/Q_t). In addition, in the late season higher precipitation intensity correlated with an increase in the volume of event water per precipitation (V_e/P) ($R^2 = 0.49$) but did not significantly correlate with a change in pre-event water (V_{pe}/P) or total runoff ratio (RR).

Localized erosion had little correlation with any significant runoff response during the early season. However, during the late season storms, net volume change (NVC) was negatively correlated with both the overall runoff ratio (RR) ($R^2 = 0.53$) and the volume of pre-event water per precipitation (V_{pe}/P) ($R^2 = 0.61$). The negative correlation of net volume change can also be expressed as a positive correlation with more erosion.

Table 3. Linear least-square regression coefficient of determination (R^2) between hydrologic response variables and the storm and basin characteristic data of NVC, Mod. B.S., High B.S., RR, I_{15}, AP_{10}, AP_5, P. The direction of the trend is shown in parentheses. Underlined values have significant correlation p-values of $p < 0.05$ and bold values $p < 0.01$.

Data Set	Comparison Value	Hydrologic Response					
		RR	V_e/P	V_{pe}/P	V_{pe}/V_{st}	Q_e/Q_t	Q_{pe}/Q_t
Entire Season	NVC	0.05 (-)	0.00 (-)	0.05 (-)	0.07 (-)	0.00 (-)	0.00 (+)
	Mod. B.S.	0.04 (-)	0.01 (-)	0.04 (-)	0.01 (-)	0.00 (-)	0.00 (-)
	High B.S.	0.02 (+)	0.00 (+)	0.02 (+)	0.01 (+)	0.00 (+)	0.00 (+)
	RR	**1.00 (+)**	**0.39 (+)**	**0.94 (+)**	0.03 (+)	0.03 (+)	<u>0.16 (+)</u>
	I_{15}	0.00 (-)	0.03 (+)	0.00 (-)	<u>0.11 (-)</u>	**0.31 (+)**	0.09 (+)
	AP_{10}	<u>0.18 (+)</u>	0.09 (+)	<u>0.16 (+)</u>	0.00 (-)	0.01 (+)	0.06 (+)
	AP_5	<u>0.15 (+)</u>	0.06 (+)	<u>0.14 (+)</u>	0.00 (+)	0.00 (+)	0.06 (+)
	P	<u>0.15 (+)</u>	0.09 (+)	<u>0.12 (+)</u>	0.00 (-)	0.01 (+)	0.02 (+)
Early Season	NVC	0.03 (-)	0.04 (-)	0.02 (-)	0.06 (-)	<u>0.36 (-)</u>	0.01 (-)
	Mod. B.S.	0.01 (-)	0.13 (-)	0.00 (-)	0.00 (+)	<u>0.35 (-)</u>	0.01 (-)
	High B.S.	0.00 (+)	0.07 (+)	0.00 (-)	0.01 (-)	<u>0.31 (+)</u>	0.00 (+)
	RR	**1.00 (+)**	0.25 (+)	**0.94 (+)**	0.22 (+)	0.00 (+)	0.17 (+)
	I_{15}	0.03 (-)	0.04 (-)	0.01 (-)	0.00 (+)	<u>0.31 (+)</u>	**0.52 (+)**
	AP_{10}	0.01 (-)	0.24 (-)	0.00 (-)	0.08 (+)	0.13 (-)	0.21 (+)
	AP_5	0.01 (-)	0.25 (-)	0.00 (+)	0.08 (+)	0.20 (-)	0.16 (+)
	P	0.00 (+)	0.00 (+)	0.00 (+)	0.00 (-)	0.08 (-)	0.02 (-)
Late Season	NVC	**0.53 (-)**	0.00 (-)	**0.60 (-)**	0.05 (-)	0.05 (+)	0.05 (+)
	Mod. B.S.	0.31 (-)	0.03 (+)	<u>0.50 (-)</u>	0.13 (-)	0.03 (+)	0.01 (-)
	High B.S.	0.20 (+)	0.07 (-)	<u>0.40 (+)</u>	0.18 (+)	0.03 (-)	0.02 (+)
	RR	**1.00 (+)**	0.16 (+)	**0.78 (+)**	0.00 (-)	0.08 (+)	0.01 (+)
	I_{15}	0.15 (+)	**0.48 (+)**	0.00 (+)	<u>0.40 (-)</u>	**0.9 (+)**	0.29 (+)
	AP_{10}	<u>0.40 (-)</u>	<u>0.34 (-)</u>	0.16 (-)	0.21 (+)	0.24 (-)	0.00 (-)
	AP_5	<u>0.34 (-)</u>	0.27 (-)	0.14 (-)	0.15 (+)	0.17 (-)	0.00 (-)
	P	0.23 (-)	0.12 (-)	0.12 (-)	0.06 (+)	0.00 (+)	0.04 (+)

Larger areas of high burn severity (High B.S.) followed similar patterns as local erosion. In the late season, sensor contributing areas that had higher amounts of high burn severity areas correlated with an increase in pre-event water per precipitation (V_{pe}/P). Areas with higher amounts of moderate burn severity area (Mod. B.S.) followed the opposite pattern, correlating with a decrease in pre-event water per precipitation (V_{pe}/P). It should be noted that net volume change (NVC) has a strong negative (or positive for erosion) correlation with High B.S. ($R^2 = 0.52$) and a strong positive (or negative for erosion) relationship with Mod. B.S. ($R^2 = 0.65$).

DISCUSSION

The results for the entire season show disparities between storms and sensor locations with few significant correlations. Some of this is likely due the 8 July storm (Storm 4) which was significantly different in storm characteristic from the other storms during the period of record. This 8 July storm produced double the runoff volume of the other storms and shifted the seasonal recession trend of the hydrograph at each site. However, seasonal differences in correlations are observed when the data are segregated between the early-season and late-season events. Early-season storms (Storms 1, 2, and 3) occurred at the beginning of hydrograph in June, before the baseflow recedes below 50% of the baseflow seen at the beginning of the season. Late-season storms (Storms 5, 6, and 7) occurred between August and October, after the baseflow as receded below 50% of the early June baseflow. In late-season storms, event water (V_e/P) and total runoff (RR) decrease with antecedent precipitation and increase with intensity. Pre-event water and total runoff increase with local erosion and high burn severity. In the early season, pre-event water peaks (Q_{pe}/Q_t) increase with higher storm intensity and event water peaks (Q_e/Q_t) are weakly correlated to intensity, burn severity, and erosion. However, volumes of runoff response (RR, V_e/P, V_{pe}/P) in the early season are not significantly correlated with net volume change, burn severity, storm intensity, or antecedent precipitation.

These results may be explained through the conceptual model depicted in Figures 5 and 6. In this model, the gradient of the near-channel water table dynamically alters the runoff response by changing the amount of stored pre-event water that becomes runoff as a result of precipitation. In the late season, the water table has been depleted through sustained baseflow with limited precipitation throughout the season and the gradient from the water table and the stream level is low. With these conditions, the amount of pre-event water that is displaced during storm events to become runoff is significantly less per unit of precipitation in the late season than the early season. Because of this, in the late season, in situations when more of the precipitation is able to infiltrate the water table, both the volume of event water per precipitation and the total runoff ratio decreases. However, when the stream channel erodes, it

18

lowers the elevation of the stream's intersection with the groundwater table, so the near-stream groundwater table gradient becomes locally high, effectively replicating the more widespread steep near-stream groundwater table of the early season. Because the early season already has a steeper gradient of groundwater table to the stream, local erosion has no effect on the groundwater table gradient and therefore the amount of pre-event water that becomes runoff per precipitation.

Antecedent Moisture

Antecedent moisture, characterized by the 5-day and 10-day volumes of precipitation that preceded the storm event (AP_5, AP_{10}), affects the runoff characteristics of the basin in disparate ways depending on when in the season the storm occurs. Conceptual models in other studies show that antecedent moisture correlates with an increase total runoff ratio as well as the amount of event-water per precipitation (Litt et al, 2015; Sidle et al., 1995; Detty and McGuire 2010; von Freyberg et al., 2014). Our results suggest that in Skin Gulch, during the early season, the peaks of event water (Q_e/Q_t) increase with increasing antecedent moisture, but no significant correlations with the volumes of event or pre-event moisture exist. However, in the late season, our results indicate the opposite of this occurs: antecedent moisture correlates with a decrease in the runoff ratio (RR), and the amount of event water per precipitation (V_e/P).

To explain this, we look first at the effects of antecedent moisture on fire-affected soils, which has been shown to increase the infiltration rate and hydraulic conductivity of hydrophobic post-fire soils (Gilmour, 1968; DeBano, 2000; Ebel and Moody, 2013). In our conceptual model shown in Figure 5, antecedent moisture increases the amount of water that is infiltrated to the groundwater, thereby decreasing the amount of precipitation that occurs as event water. However, although more event water is infiltrated to the groundwater, the gradient of the near-stream groundwater table is low so additional pre-event water is not displaced from the groundwater table at the same rate that event water is decreased. This causes a decrease the total runoff ratio as well as event water per precipitation, with an increase in pre-event water, which is supported by our results.

In contrast, in the early season, the near-stream groundwater table gradient is already steep, especially in the alluvial floodplain, because the overall groundwater level is high. In these conditions, saturation excess of the interflow zone may be either preventing more precipitation from infiltrating, or causing interflow zone water to exfiltrate and become surface runoff (Sophocleous, 2002). Consequently, during the early season, the total volumes of pre-event and event water are not significantly altered by the increased permeability of the surface layer and so no significant correlation with volume exists.
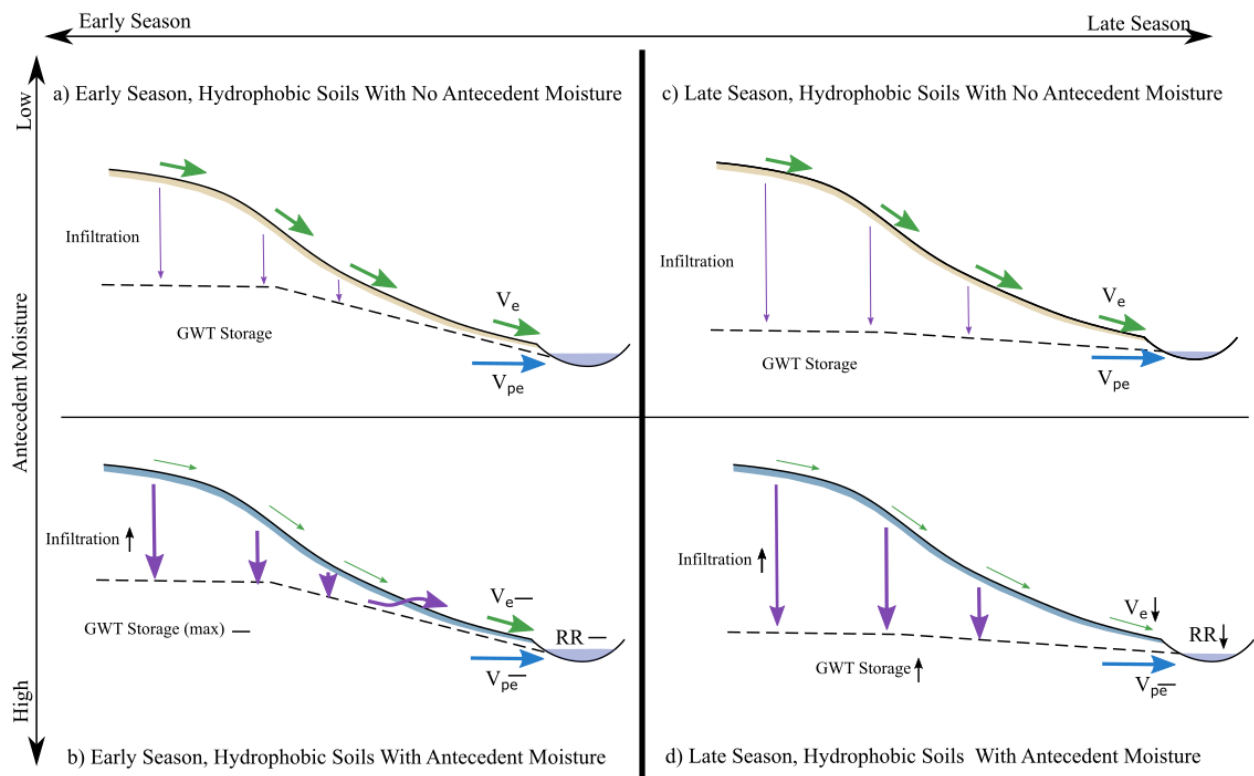
Figure 5. *Conceptual model of how the depth to groundwater table and antecedent moisture can decrease the event water (V_e/P) and total runoff (RR) in the late season. c) shows late season conditions with no antecedent moisture and hydrophobic soils at the surface. d) shows how when antecedent moisture increases the infiltration capacity of the hydrophobic soils event runoff (V_e) is decreased, but due to low groundwater table gradient the pre-event runoff (V_{pe}) is not increased by a corresponding amount, lowering the overall runoff ratio (RR) a) and b) show the same scenario but with early season high groundwater table conditions allowing excess infiltration to return surface flow, thereby not affecting the volumes of event or pre-event water (V_e to V_{pe}) or the total amount of runoff (RR).*

Precipitation Intensity

Precipitation intensity has been linked to increased runoff ratio and increased event water per precipitation in multiple studies (Pellerin, 2006; von Freyberg, 2018). In Skin Gulch the runoff response

to precipitation intensity changes from the early season to the late season. In the late season, higher precipitation intensity correlates with increased event water per precipitation (V_e/P). This response has been seen in other studies (von Freyberg, 2018; Pellerin et al., 2008; Waddington et al. 1993) and is generally explained by high rainfall intensity overwhelming infiltration capacity and resulting in greater surface water runoff. In our study, precipitation intensity is also highly correlated with higher event water peaks in the late season, which is consistent with this interpretation.

In the early season, increasing intensity only correlates with the relative peaks of both event water and pre-event water (Q_e/Q_t, Q_{pe}/Q_t), increasing both, and may be explained simply by the fact that higher precipitation peaks will result in larger runoff peaks and less sustained runoff. Unlike in the late season though, in the early-season storms the overall volumes of event water and pre-event water per precipitation (V_e/P, V_{pe}/P) are not correlated with precipitation intensity. This may be due to the fact that the early season storms also had less variation of precipitation intensity between storms than in the late season, making significant correlations more difficult to find.

Net Sediment Volume Change (NVC)

As far as we are aware, the effect of localized channel erosion on runoff response has not been studied in detail previously. However, other work on stream gains and losses has suggested that groundwater contributions to the stream can vary based on local topography (Harvey et al., 1996; Kasahara and Wondzell, 2003), and we find results here that suggest this is true for localized net sediment volume changes (*NVC*) in the stream corridor. Similar to the other controls on runoff generation examined in this study, the correlation with localized erosion is disparate based on whether the event occurs in the early or late season. In the early season, sites with local net erosion were only correlated with an increase in the relative peak of event runoff. In the late season, however, locations with local erosion show a strong correlation with an increase in pre-event water per precipitation (V_{pe}/P) and total runoff per precipitation (*RR*). We hypothesize that this late-season response, and its contrast with the early-season response, can be explained the conceptual model of a lower near-stream groundwater table gradient in the late season, shown in Figure 6. We propose sites with more local erosion lower the elevation of the stream

and thereby increase the gradient of the near-stream water table. Therefore, at these sites with more local erosion, precipitation that infiltrates to the groundwater table displaces more pre-event water as runoff that sites with less erosion, and therefore a less-steep groundwater table gradient. In the early season the gradient between the water table and the stream is already high and localized erosion does not significantly increase the gradient to water table. This would result in no significant increase to pre-event water as is supported by the results.
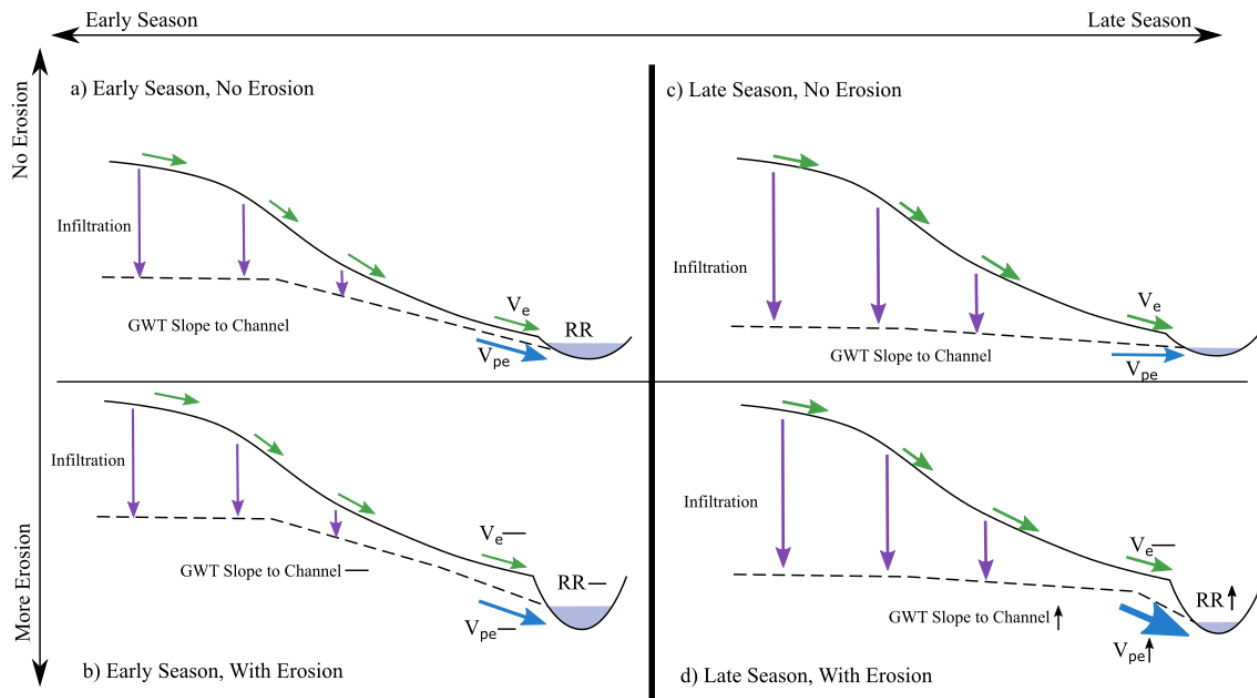
Figure 6. *Conceptual model of how the depth to groundwater table and localized erosion can affect runoff in the late season. c) shows late season conditions with no localized erosion and a low gradient groundwater table d) shows how localized erosion can increase both the total runoff ratio (RR) and pre-event runoff (V_{pe}) by increasing the gradient of the water table to the stream. a) and b) show the same scenario in the early season, when ground water table gradient is already high. In d) event and pre-event runoff (V_e and V_{pe}) along with total runoff ration (RR) remains the same since the localized erosion does not significantly increase the already steep gradient of the groundwater table.*

Due to the nested nature of our sensor locations, the fact that this late season correlation between erosion ($NVC < 0$) and pre-event water is observable shows that this effect is highly localized, and local erosion does not increase pre-event water relative to precipitation at downstream sensor sites, which experienced less erosion or even deposition ($NVC > 0$, see Figure 1). This suggests that, in locations

where no erosion, or net deposition, occurred, the pre-event water may be removed from the runoff signature in the stream and resupply the groundwater table at that location.

Burn Severity

High burn severity (High B.S.) is correlated with an increase pre-event water (V_{pe}/P) in the same way that net volume change (NVC) is; moderate burn severity (Mod B.S.) is correlated with a decrease in pre-event water, and both have similar strength of correlations. High B.S. and Mod. B.S. are themselves correlated with NVC which suggests that areas with High B.S. are more likely to have significant local erosion (or negative NVC), and areas with more Mod. B.S. are less likely to have erosion. Increased burn severity is typically associated with an increase is surface runoff or event water due to changes in soil properties and vegetation. However, at Skin Gulch the opposite is true, as in late-season storms the percent high burn severity was significantly correlated with pre-event water in the runoff. This suggests that despite the effects of higher burn severity to soil and vegetation, the localized erosion, and therefore the local gradient of the groundwater table to the stream, has a much larger role in the composition of runoff.

Discussion Summary

We have discussed seasonal changes to the correlations between hydrologic response and antecedent moisture, precipitation intensity, local erosion and burn severity. Pre-event water (V_{pe}/P) and total runoff (RR) decrease with antecedent moisture, but only when the groundwater table gradient is low (late season). Higher precipitation intensity increases the volume of event water (V_e/P) and total runoff (RR) when the groundwater table gradient is low (late season). When the groundwater table gradient is high (early season), only the relative peaks of the event water runoff (Q_e/P) are affected by precipitation intensity, and no volumes are correlated. Pre-event water (V_{pe}/P) and total runoff (RR) are also increased by local erosion of sediment in the stream corridor, but only when the existing groundwater table is low, suggesting that the erosion of the stream bed increases the local slope of the groundwater table to the stream.

CONCLUSIONS, AND FUTURE WORK

Separating storm hydrographs into event water and pre-event water for 7 storms across 6 sites in a burned and disturbed mountain catchment revealed correlations with antecedent precipitation, precipitation intensity, and net geomorphic channel change. These correlations vary based on whether they occur in the early-season portion of the summer or the late-season portion. We hypothesize that the near-stream gradient of the water table as well as fire-affected hydrophobic soils are part of the explanation behind the disparate results. In the late season, antecedent moisture decreases total runoff and event water per precipitation, while the pre-event water per precipitation remains the same. Higher precipitation intensity increases the event water per precipitation as well as the total runoff, but only in the late season. Finally, our results suggest that localized erosion plays a role in how much pre-event water per precipitation occurs at a site, by potentially increasing the groundwater table gradient to the stream.

In general, our results show stronger correlations with effects of antecedent moisture, rainfall intensity and net geomorphic volume change during the late season, when we speculate that the gradient of the groundwater table to the stream is low. These results suggest that the gradient of the water table can create conditions where the distribution of event and pre-event water is more sensitive to site and storm characteristics than they would be during early season conditions with a higher groundwater table.

Our findings could be strengthened with additional seasons of data, and a series of groundwater depth sensors could corroborate the hypothesis that the gradient of the groundwater is behaving as our conceptual models suggest. Our results suggest that future studies on the runoff characteristics following a wildfire should consider not only direct effects of the fire, like hydrophobic soils, but also subsequent effects and changes to the geomorphology and topography like recent channel erosion. Additionally, seasonality may be an important consideration in hydrograph separation studies. This factor may also interact with other watershed characteristics (in this case hydrophobic soils) in unexpected ways and future studies should consider examining results based on seasonality of the events for differing results from the entire data set.

REFERENCES

Abbott, J. T. (1970). Geology of Precambrian rocks and isotope geochemistry of shear zones in the Big Narrows area, northern Front Range, Colorado (No. 70-1). *US Geological Survey*.

Brogan, D. J., Nelson, P. A., & MacDonald, L. H. (2017). Reconstructing extreme post-wildfire floods: a comparison of convective and mesoscale events. *Earth Surface Processes and Landforms*, 42(15), 2505-2522.

Brogan, D. J., MacDonald, L. H., Nelson, P. A., & Morgan, J. A. (2019a). Geomorphic complexity and sensitivity in channels to fire and floods in mountain catchments. *Geomorphology*, 337, 53-68.

Brogan, D. J., Nelson, P. A., & MacDonald, L. H. (2019b). Spatial and temporal patterns of sediment storage and erosion following a wildfire and extreme flood. *Earth Surface Dynamics*, *7*(2), 563-590.

Cano-Paoli, K., Chiogna, G., & Bellin, A. (2019). Convenient use of electrical conductivity measurements to investigate hydrological processes in Alpine headwaters. *Science of The Total Environment*, *685*, 37-49.

Day, T. J. (1976). On the precision of salt dilution gauging. *Journal of Hydrology*, *31*(3-4), 293-306.Debano, 2000

DeBano, L. F. (2000). The role of fire and soil heating on water repellency in wildland environments: a review. *Journal of hydrology*, *231*, 195-206.

D'Errico, John (2021) SLM - Shape Language Modeling (https://www.mathworks.com/matlabcentral/fileexchange/24443-slm-shape-language-modeling), *MATLAB Central File Exchange*. Retrieved November, 2021.

Detty, J. M., & McGuire, K. J. (2010). Threshold changes in storm runoff generation at a till-mantled headwater catchment. *Water Resources Research*, *46*(7).

Ebel, B. A. (2012). Wildfire impacts on soil-water retention in the Colorado Front Range, United States. *Water Resources Research*, *48*(12).

Ebel, B. A., & Moody, J. A. (2013). Rethinking infiltration in wildfire-affected soils. *Hydrological Processes*, *27*(10), 1510-1514.

Engel, M., Penna, D., Comiti, F., Vignoli, G., Simoni, S., & Dinale, R. (2016, April). Tracing the spatial and temporal variability of different water sources in a glacierized Alpine catchment (Eastern Italian Alps). In *EGU General Assembly Conference Abstracts* (pp. EPSC2016-14920).

von Freyberg, J., Studer, B., Rinderer, M., & Kirchner, J. W. (2018). Studying catchment storm response using event-and pre-event-water volumes as fractions of precipitation rather than discharge. *Hydrology and Earth System Sciences*, *22*(11), 5847-5865.

Gilmour, D. A. (1968). Water repellence of soils related to surface dryness. *Australian forestry*, *32*(3), 143-148.

Harvey, J. W., Wagner, B. J., & Bencala, K. E. (1996). Evaluating the reliability of the stream tracer approach to characterize stream-subsurface water exchange. *Water resources research*, *32*(8), 2441-2451.

Hudson, R., & Fraser, J. (2005). The mass balance (or dry injection) method. *Streamline Watershed Management Bulletin*, *9*(1), 6-12.

Imeson, A. C., Verstraten, J. M., Van Mulligen, E. J., & Sevink, J. (1992). The effects of fire and water repellency on infiltration and runoff under Mediterranean type forest. *Catena*, *19*(3-4), 345-361.

Inamdar, S., Dhillon, G., Singh, S., Dutta, S., Levia, D., Scott, D., ... & McHale, P. (2013). Temporal variation in end-member chemistry and its influence on runoff mixing patterns in a forested, Piedmont catchment. *Water Resources Research*, *49*(4), 1828-1844.

Kampf, S. K., Brogan, D. J., Schmeer, S., MacDonald, L. H., & Nelson, P. A. (2016). How do geomorphic effects of rainfall vary with storm type and spatial scale in a post-fire landscape?. *Geomorphology*, *273*, 39-51.

Kasahara, T., & Wondzell, S. M. (2003). Geomorphic controls on hyporheic exchange flow in mountain streams. *Water Resources Research*, *39*(1), SBH-3.

Klaus, J., & McDonnell, J. J. (2013). Hydrograph separation using stable isotopes: Review and evaluation. *Journal of hydrology*, *505*, 47-64.

Kopp, B. J., Lange, J., & Menzel, L. (2017). Effects of wildfire on runoff generating processes in northern Mongolia. *Regional Environmental Change*, *17*(7), 1951-1963.

Kronholm, S. C., & Capel, P. D. (2015). A comparison of high-resolution specific conductance-based end-member mixing analysis and a graphical method for baseflow separation of four streams in hydrologically challenging agricultural watersheds. *Hydrological Processes*, *29*(11), 2521-2533.

Larsen, I. J., MacDonald, L. H., Brown, E., Rough, D., Welsh, M. J., Pietraszek, J. H., ... & Schaffrath, K. (2009). Causes of post-fire runoff and erosion: Water repellency, cover, or soil sealing?. *Soil Science Society of America Journal*, *73*(4), 1393-1407.

Laudon, H., & Slaymaker, O. (1997). Hydrograph separation using stable isotopes, silica and electrical conductivity: an alpine example. *Journal of hydrology*, *201*(1-4), 82-101.

Lott, D. A., & Stewart, M. T. (2016). Base flow separation: A comparison of analytical and mass balance methods. *Journal of Hydrology*, *535*, 525-533.

Martin, C., Kampf, S. K., Hammond, J. C., Wilson, C., & Anderson, S. P. (2021). Controls on streamflow densities in semiarid rocky mountain catchments. *Water*, *13*(4), 521.

Matsubayashi, U., Velasquez, G. T., & Takagi, F. (1993). Hydrograph separation and flow analysis by specific electrical conductance of water. *Journal of Hydrology*, *152*(1-4), 179-199.

McDonnell, J. J. (1990). A rationale for old water discharge through macropores in a steep, humid catchment. *Water Resources Research*, *26*(11), 2821-2832.

McGuire, L. A., & Youberg, A. M. (2019). Impacts of successive wildfire on soil hydraulic properties: Implications for debris flow hazards and system resilience. *Earth Surface Processes and Landforms*, *44*(11), 2236-2250.

Moore, R. D. (2005). Slug injection using salt in solution. *Streamline Watershed Management Bulletin*, *8*(2), 1-6.

National Atmospheric Deposition Program (NADP) (NRSP-3). 2021. NADP Program Office, *Wisconsin State Laboratory of Hygiene,* 465 Henry Mall, Madison, WI 53706.

Pellerin, B. A., Wollheim, W. M., Feng, X., & Vörösmarty, C. J. (2008). The application of electrical conductivity as a tracer for hydrograph separation in urban catchments. *Hydrological Processes: An International Journal*, *22*(12), 1810-1818.

Pilgrim, D. H., Huff, D. D., & Steele, T. D. (1979). Use of specific conductance and contact time relations for separating flow components in storm runoff. *Water Resources Research*, *15*(2), 329-339.

Raymond, C. A., McGuire, L. A., Youberg, A. M., Staley, D. M., & Kean, J. W. (2020). Thresholds for post-wildfire debris flows: Insights from the Pinal Fire, Arizona, USA. *Earth Surface Processes and Landforms*, *45*(6), 1349-1360.

Scott, D. F. (1997). The contrasting effects of wildfire and clearfelling on the hydrology of a small catchment. *Hydrological Processes*, *11*(6), 543-555.

USDA Labratory Staff (1954). Diagnosis and Improvement of Saline and Alkali Soils. *Agriculture Handbook No. 60* USDA

Sophocleous, M. (2002). Interactions between groundwater and surface water: the state of the science. *Hydrogeology journal*, *10*(1), 52-67.

Stoof, C. R., Vervoort, R. W., Iwema, J., Van Den Elsen, E., Ferreira, A. J. D., & Ritsema, C. J. (2012). Hydrological response of a small catchment burned by experimental fire. *Hydrology and Earth System Sciences*, *16*(2), 267-285.

Weijs, S. V., Mutzner, R., & Parlange, M. B. (2013). Could electrical conductivity replace water level in rating curves for alpine streams?. *Water Resources Research*, *49*(1), 343-351.

Wilson, C., Kampf, S. K., Ryan, S., Covino, T., MacDonald, L. H., & Gleason, H. (2021). Connectivity of post-fire runoff and sediment from nested hillslopes and watersheds. *Hydrological Processes*, *35*(1), e13975.

Appendix A contains all the event hydrographs used in this analysis with each showing total discharge, baseflow, pre-event water, and event water. No Hydrographs were created for Site 1 - Storm 6, Site 1 - Storm 7, and Site 8 – Storm 7 since during the course of field measurements the stream water levels dropped below the sensor level and no measurements were taken. The hydrograph for Site 4 Storm 3 is excluded as the sensor had been temporarily removed during that time to fix a malfunction.

Site 1, Storm 1 Event Hydrograph 11-Jun

Site 1, Storm 2 Event Hydrograph 28-Jun

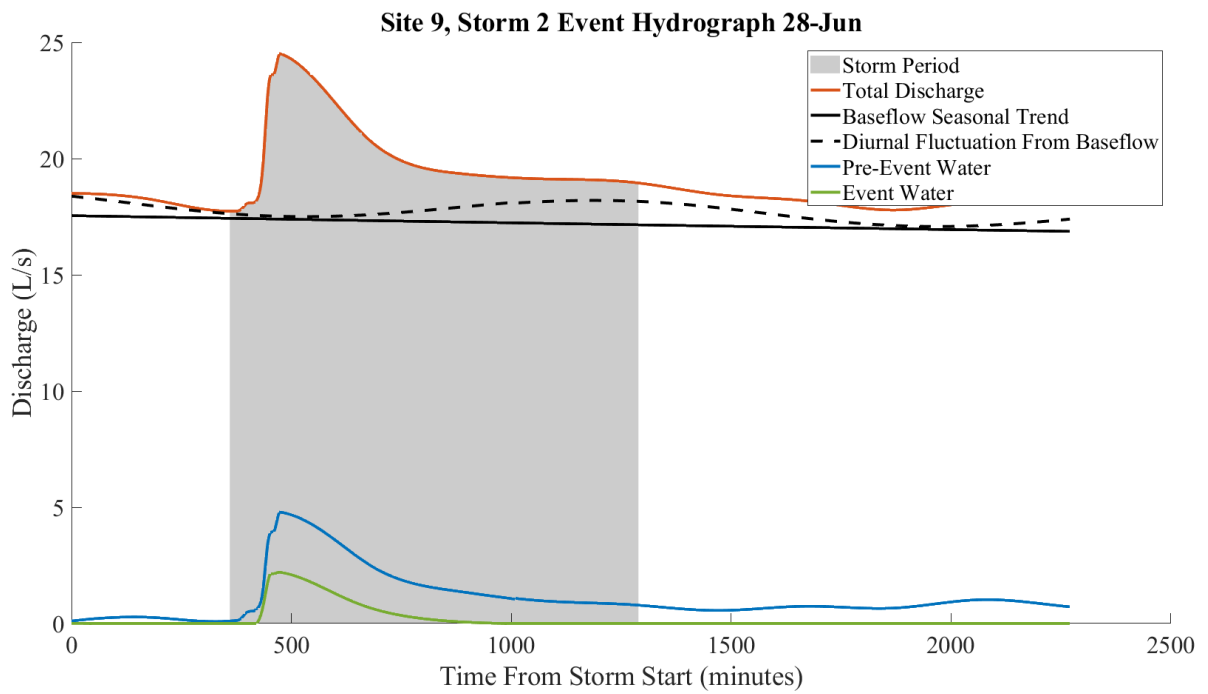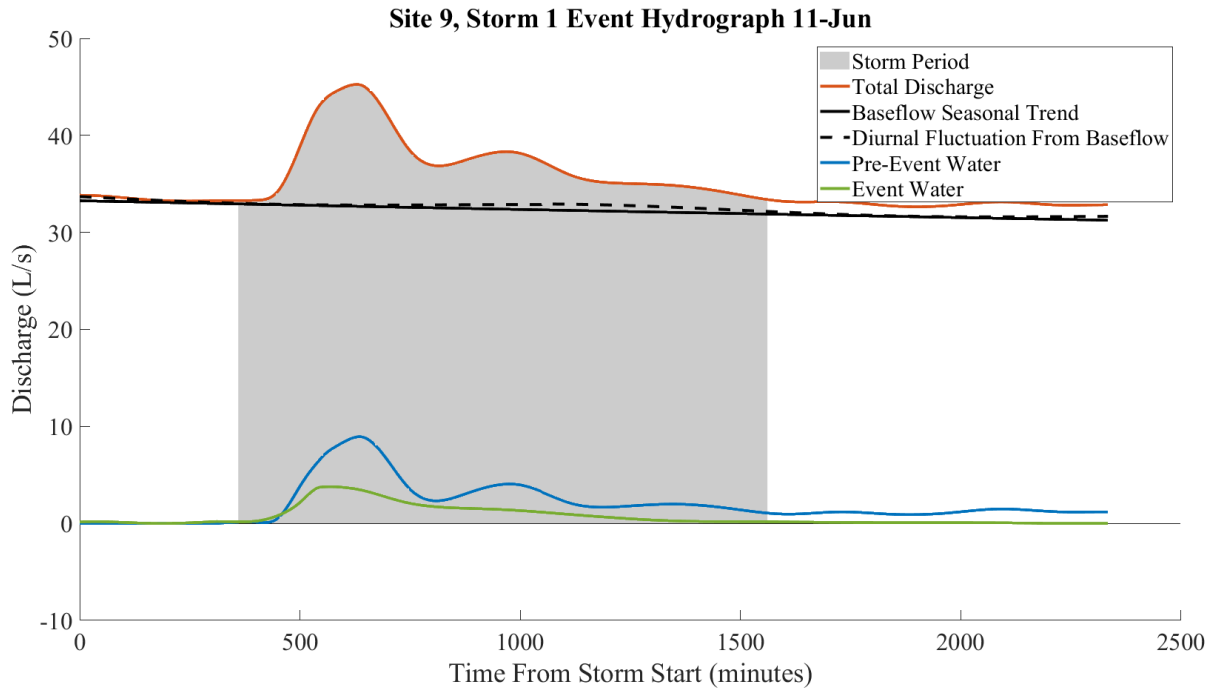**Site 1, Storm 3 Event Hydrograph 01-Jul**
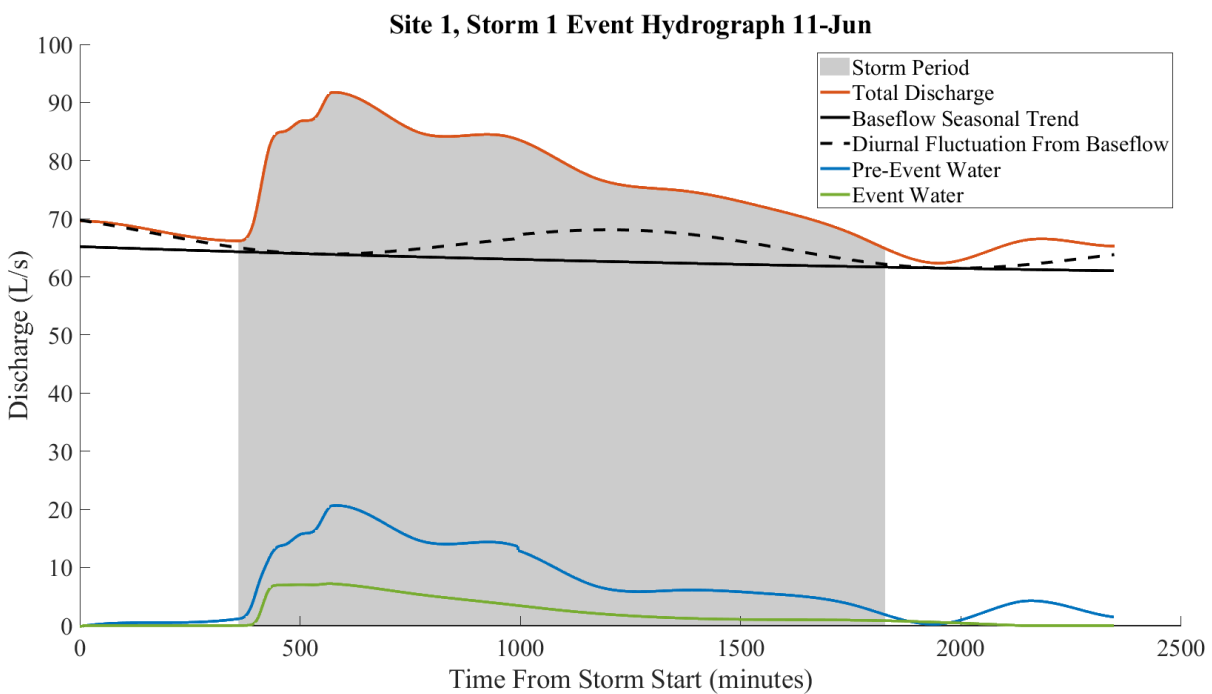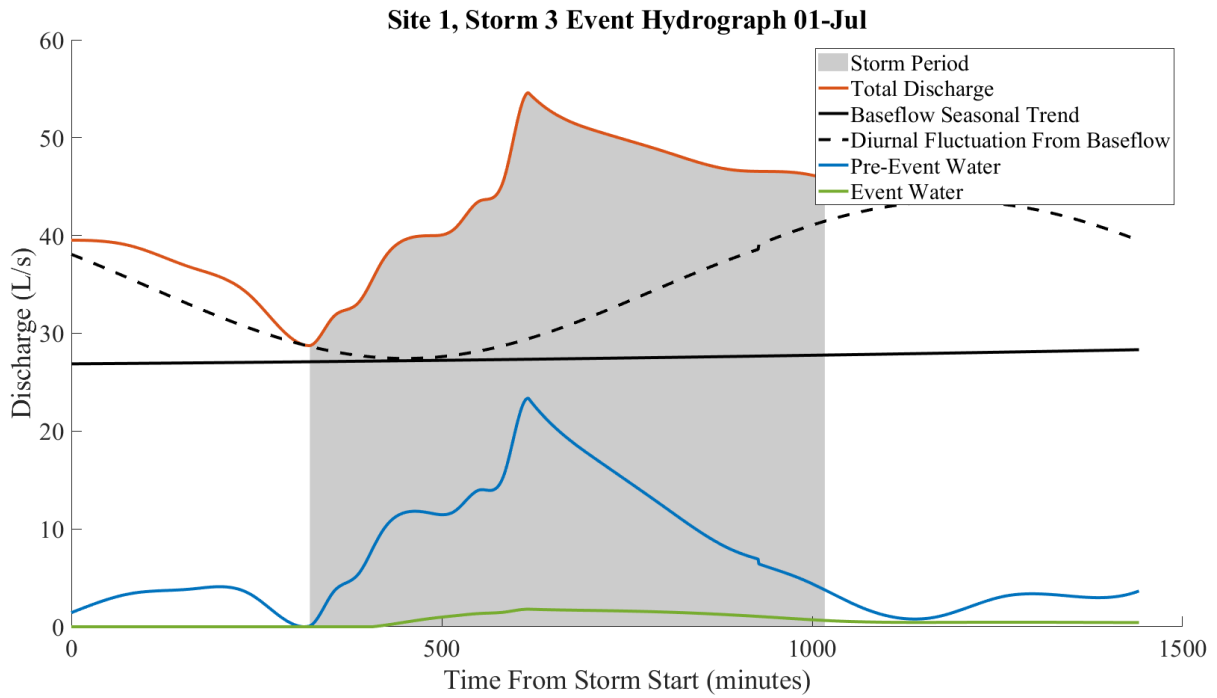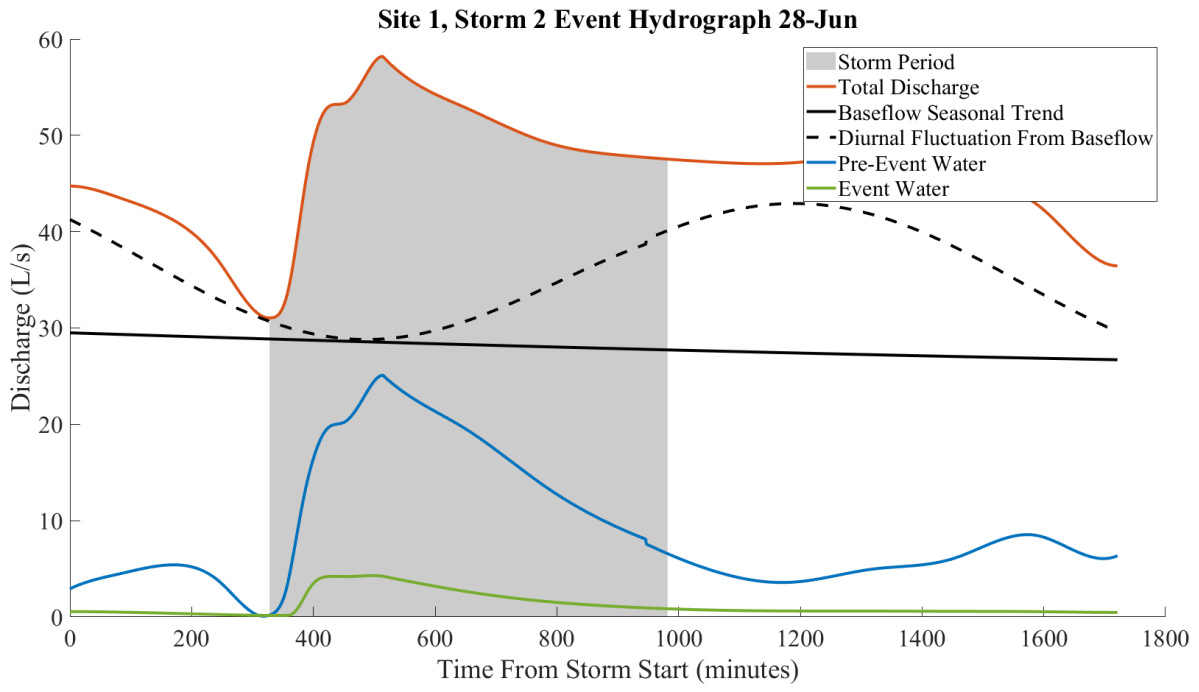
Site 1, Storm 4 Event Hydrograph 08-Jul
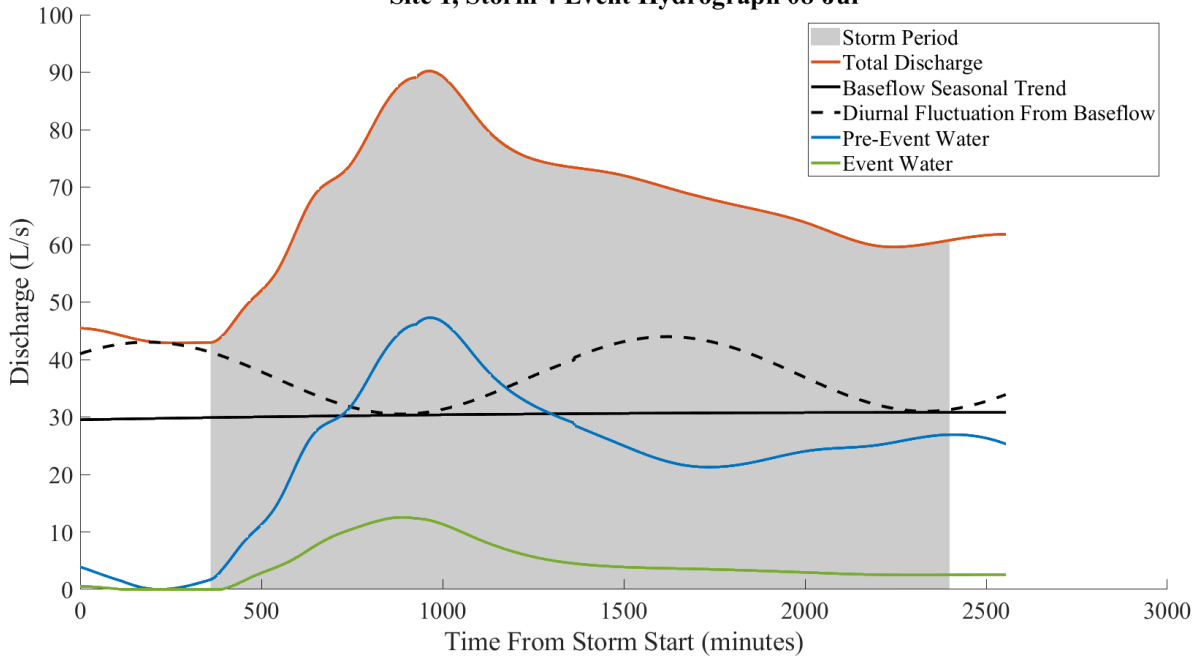
Site 1, Storm 5 Event Hydrograph 16-Aug
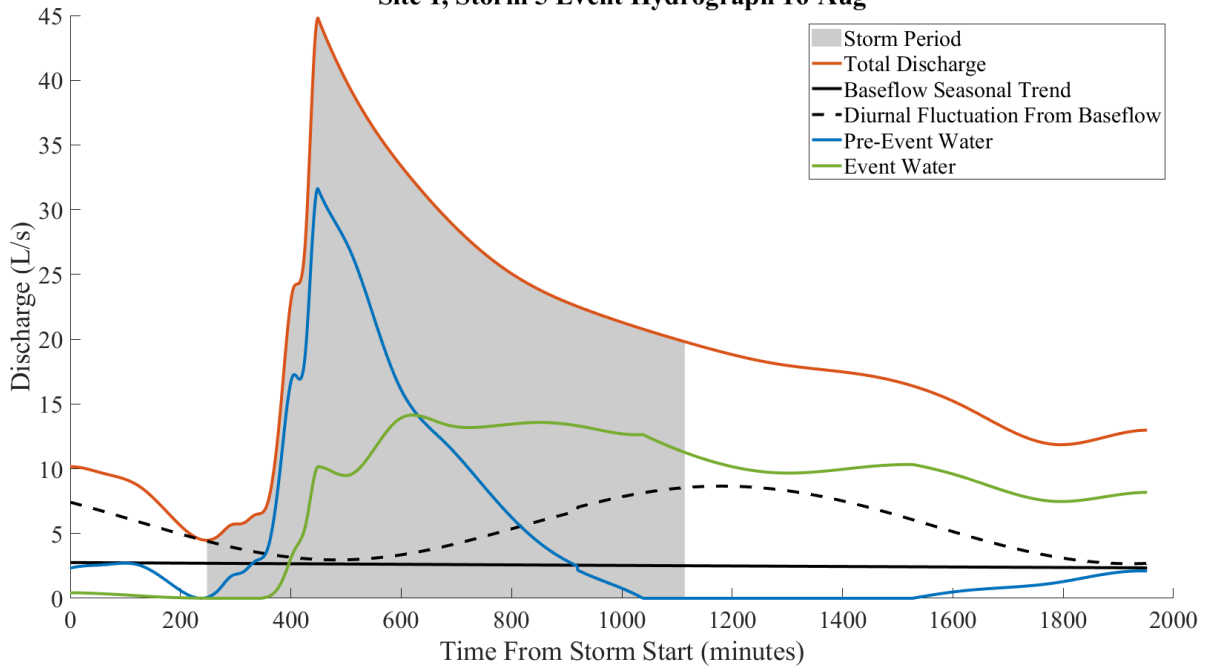
Site 3, Storm 1 Event Hydrograph 11-Jun
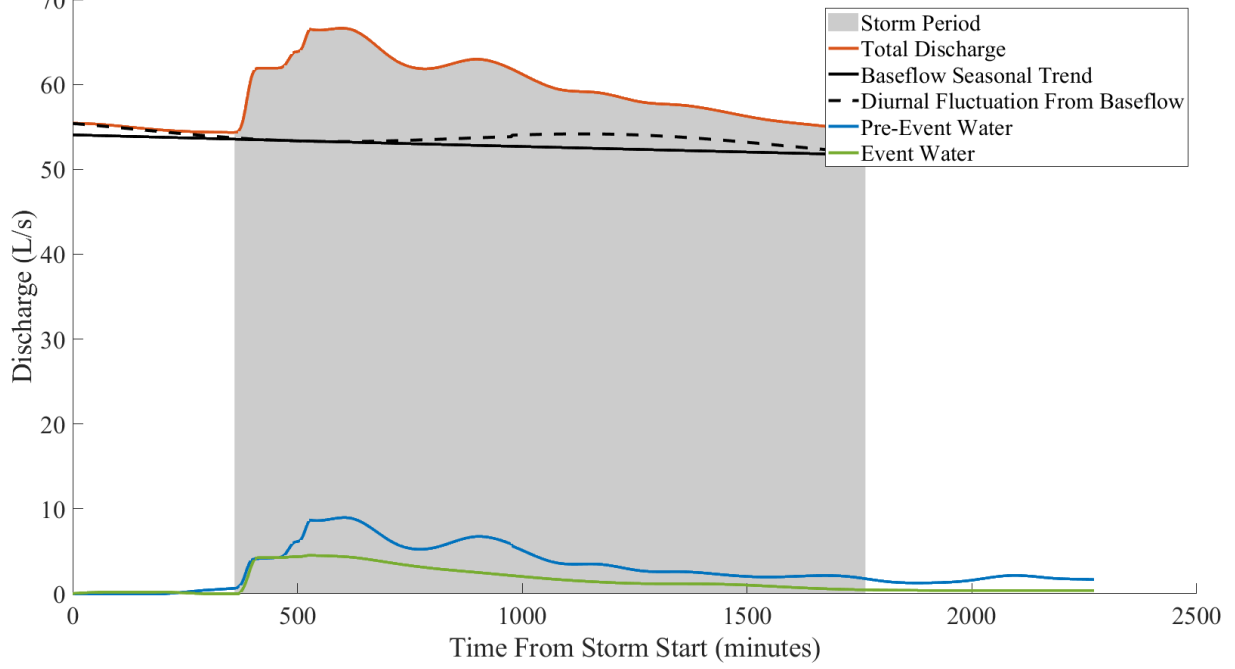
Site 3, Storm 2 Event Hydrograph 28-Jun

31
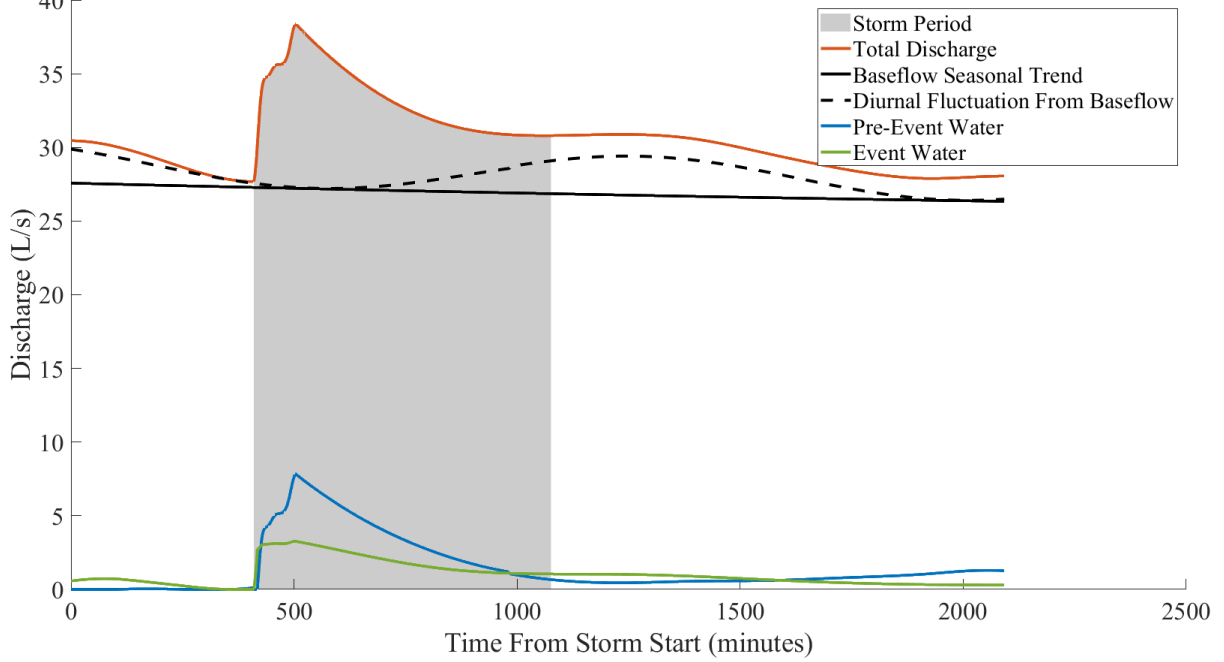
Site 3, Storm 3 Event Hydrograph 01-Jul
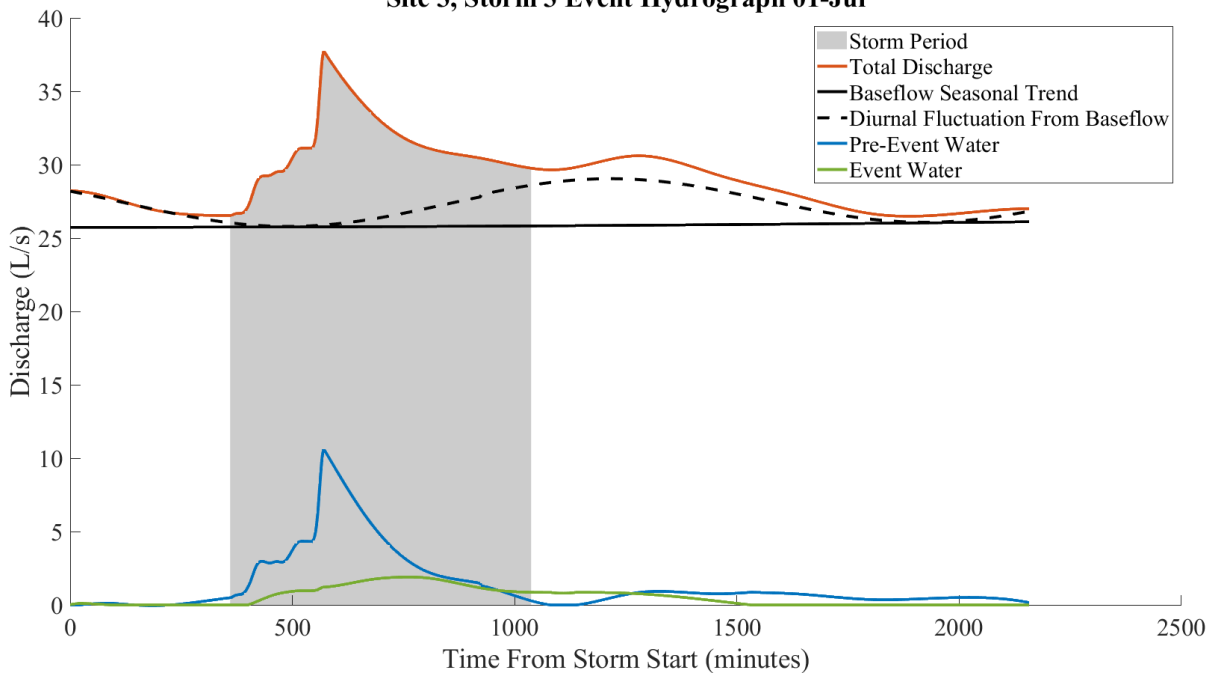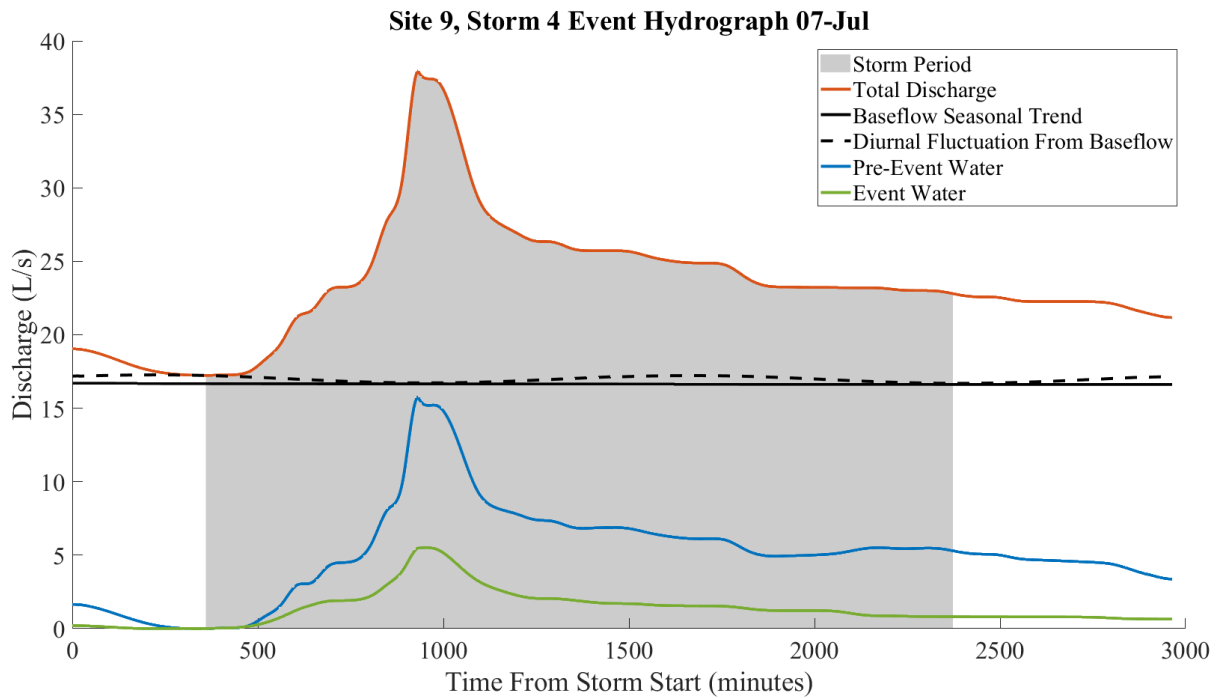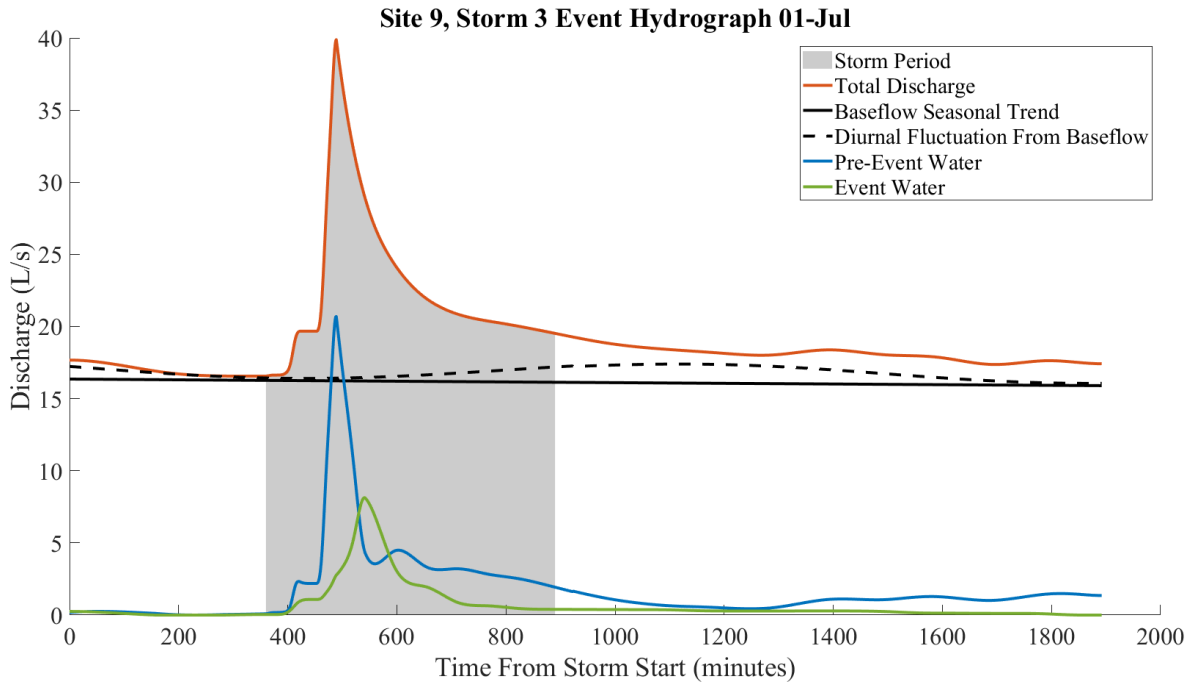

Site 3, Storm 4 Event Hydrograph 08-Jul
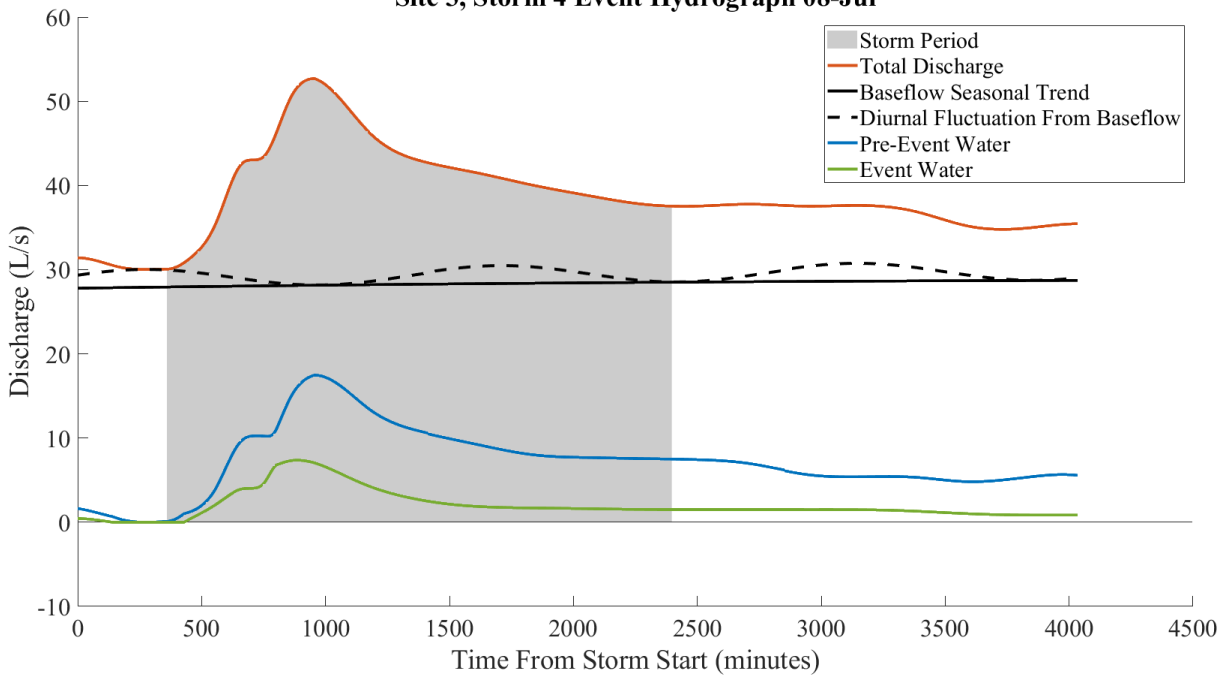
Site 3, Storm 5 Event Hydrograph 16-Aug
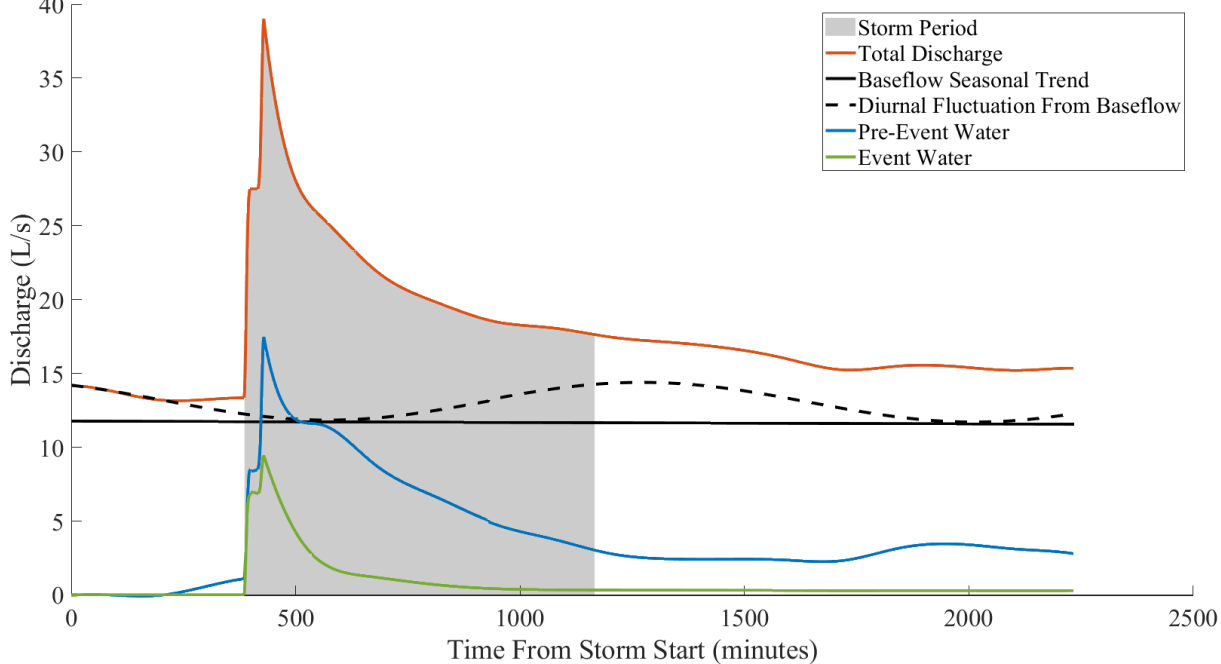
Site 3, Storm 6 Event Hydrograph 18-Aug
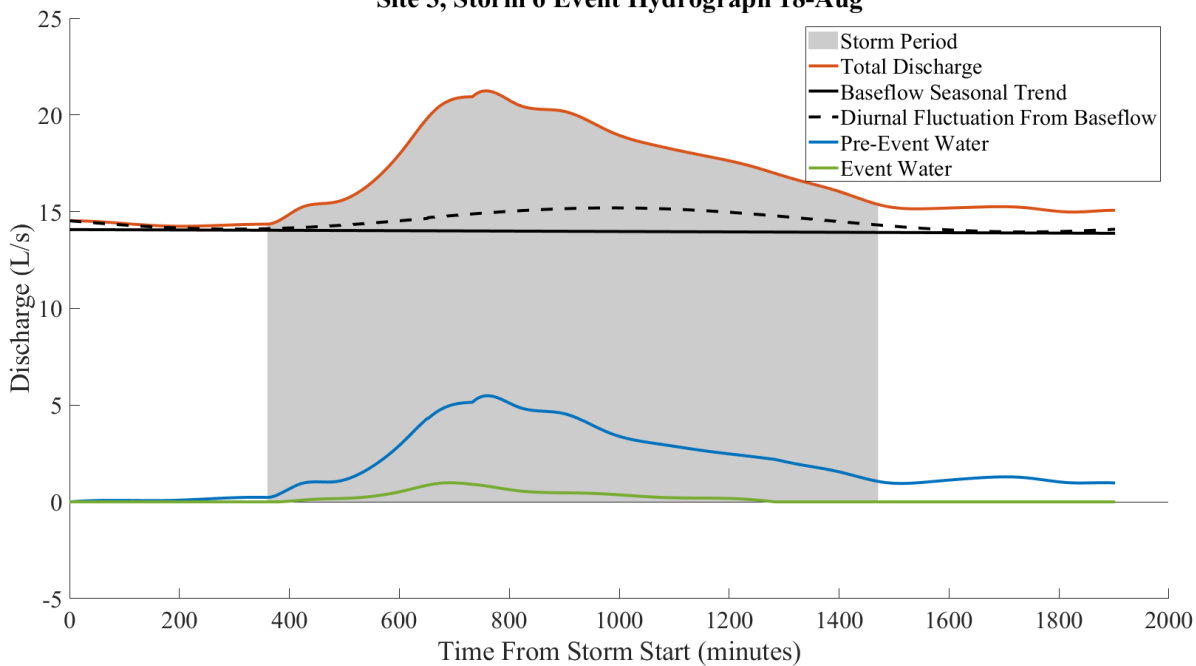
Site 3, Storm 7 Event Hydrograph 06-Oct
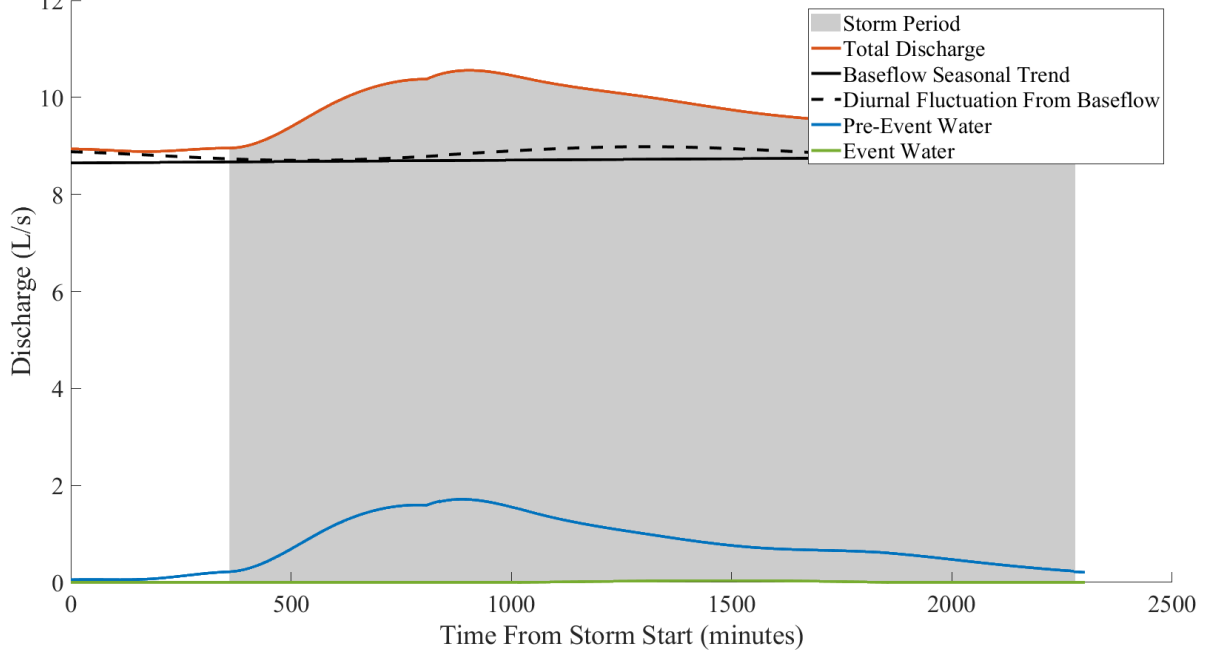
Site 4, Storm 1 Event Hydrograph 11-Jun

Site 4, Storm 2 Event Hydrograph 28-Jun

Site 4, Storm 4 Event Hydrograph 07-Jul
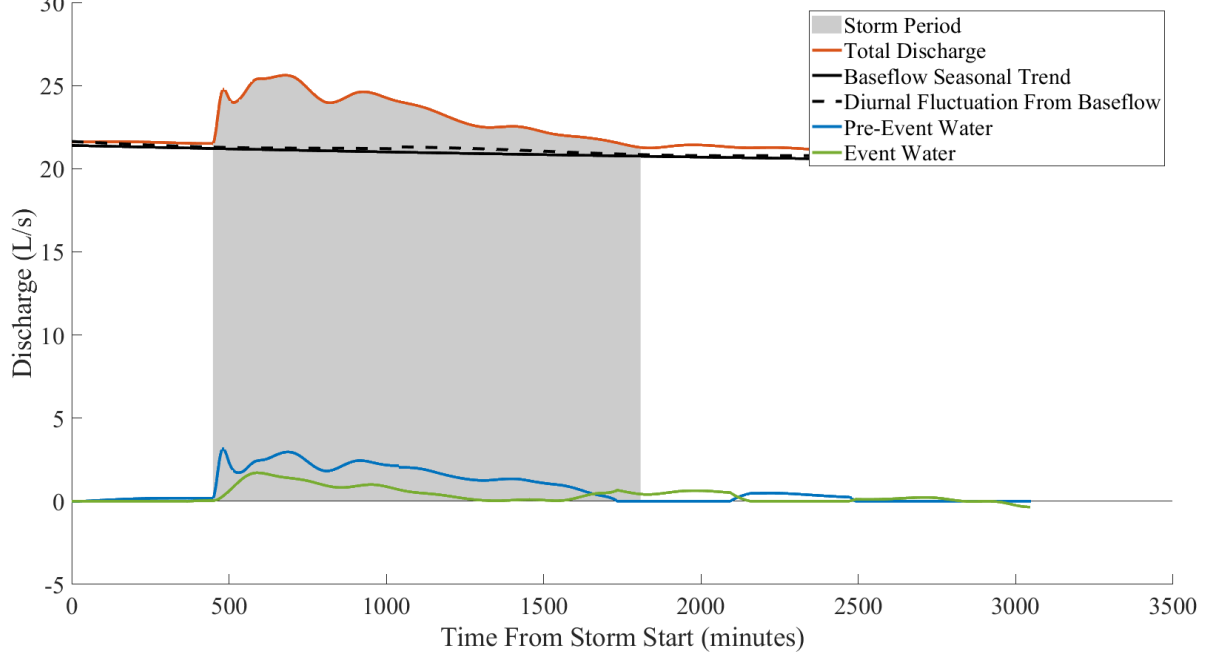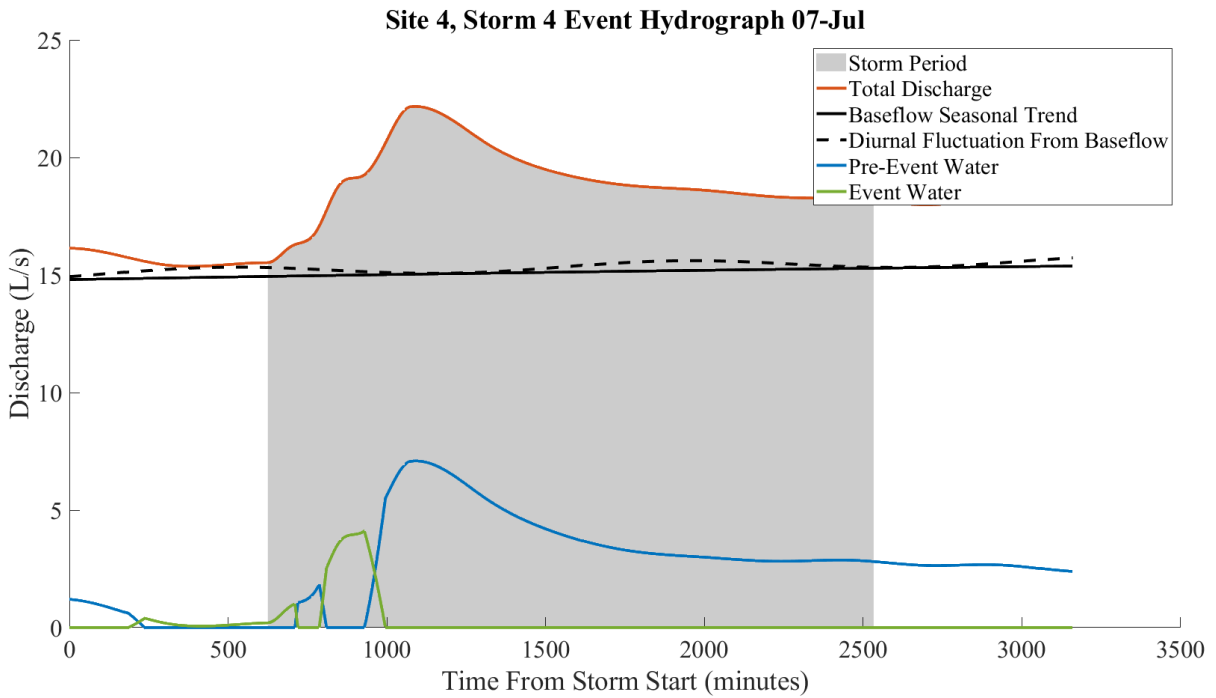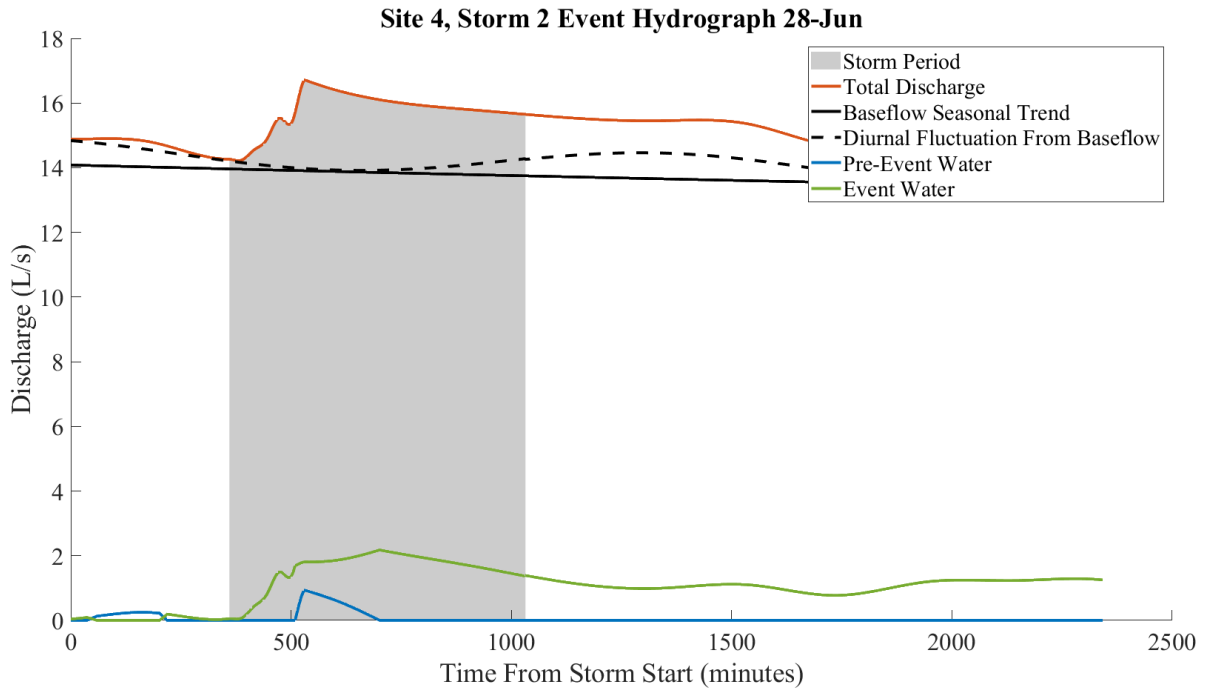
Site 4, Storm 5 Event Hydrograph 16-Aug
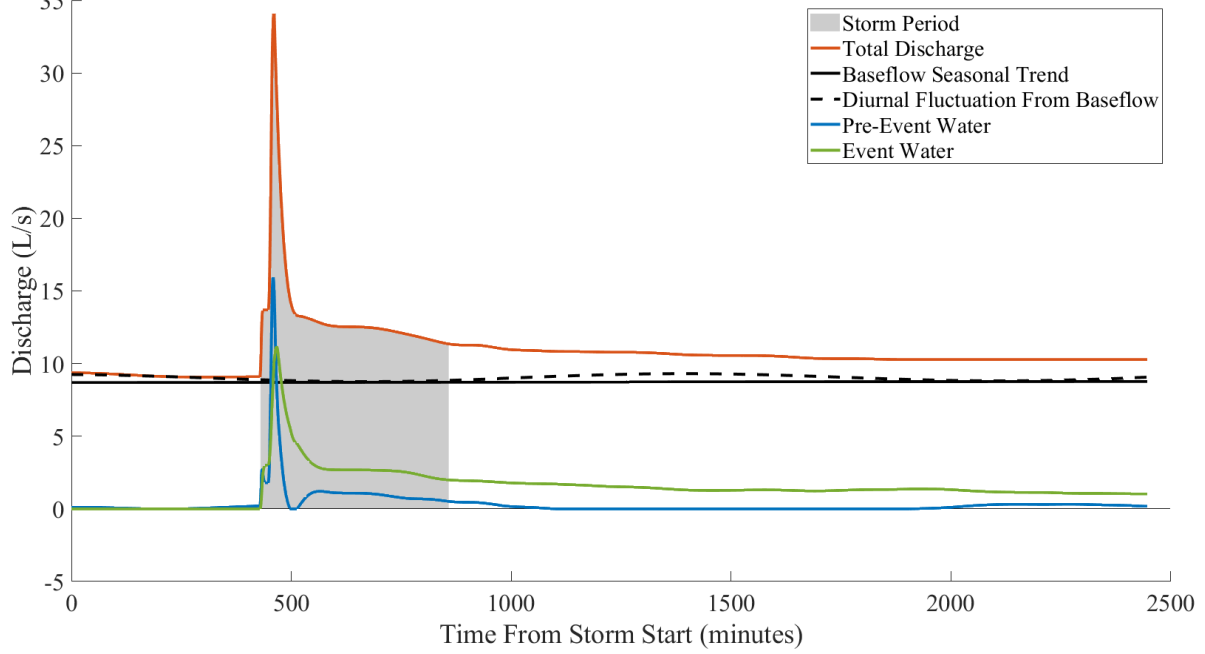
Site 4, Storm 6 Event Hydrograph 18-Aug
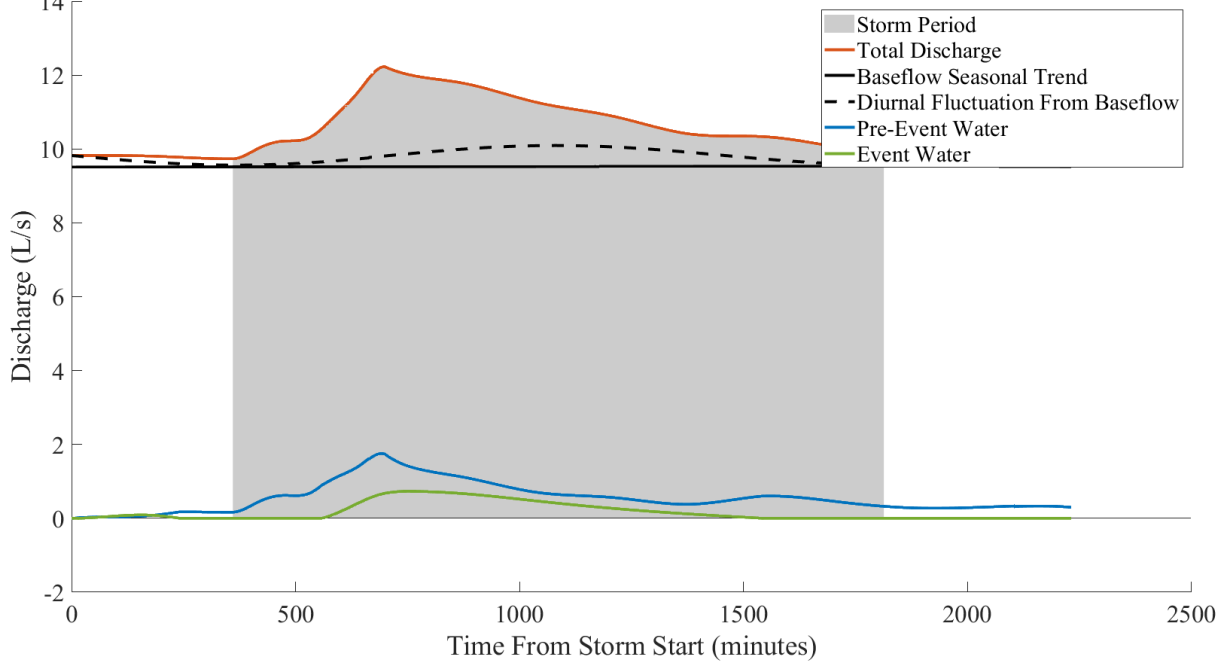
Site 4, Storm 7 Event Hydrograph 06-Oct
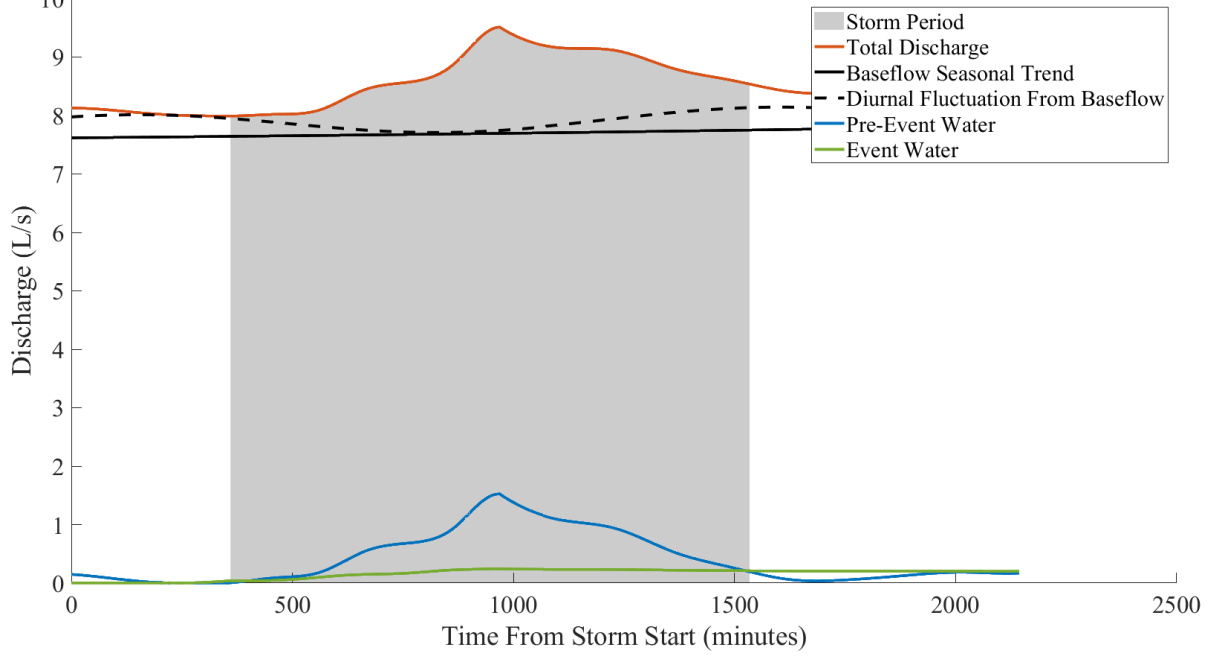
Site 5, Storm 1 Event Hydrograph 11-Jun

Site 5, Storm 2 Event Hydrograph 28-Jun

Site 5, Storm 3 Event Hydrograph 01-Jul

Site 5, Storm 4 Event Hydrograph 07-Jul

Site 5, Storm 5 Event Hydrograph 16-Aug
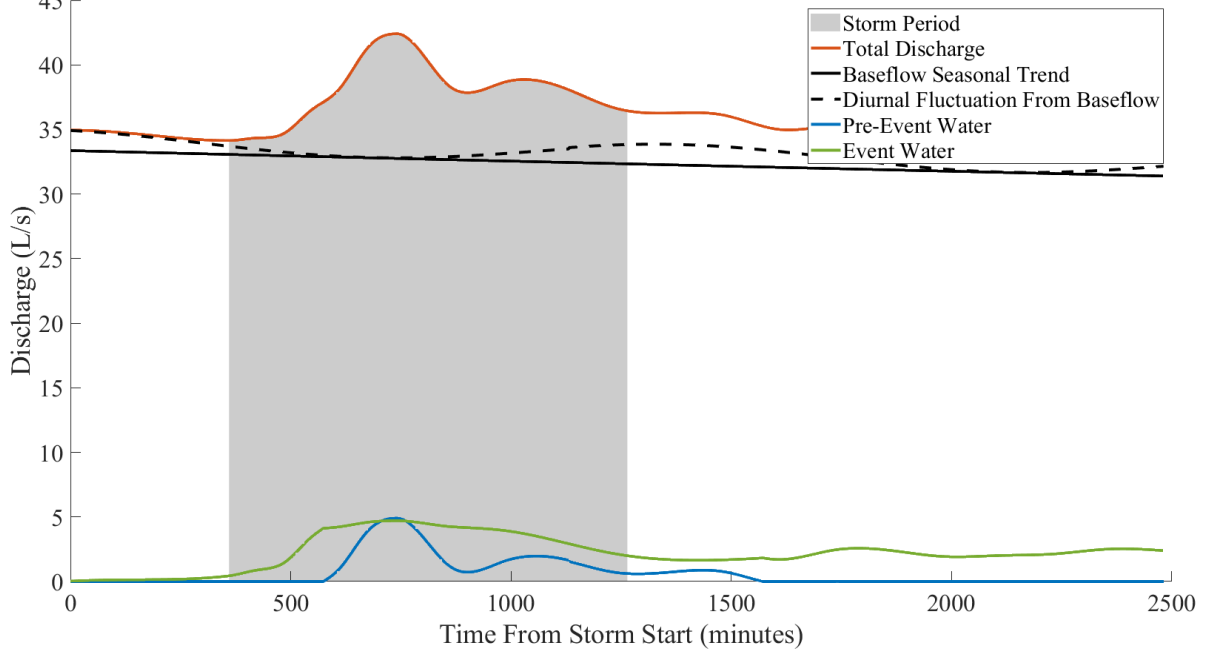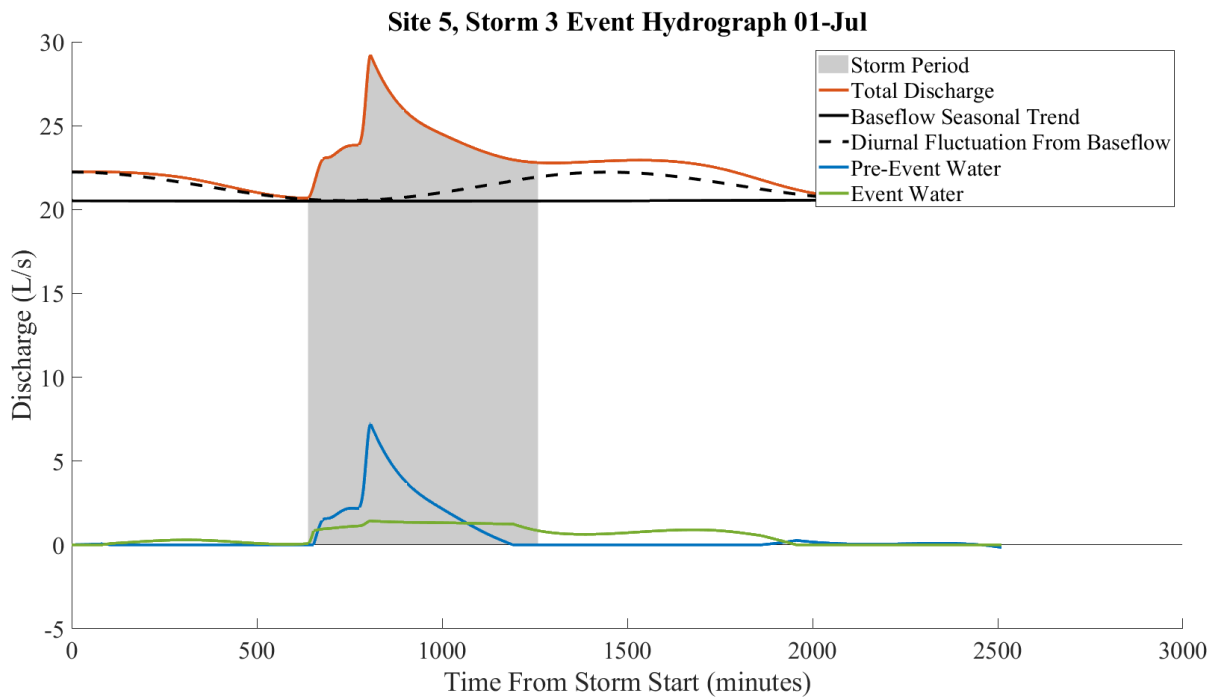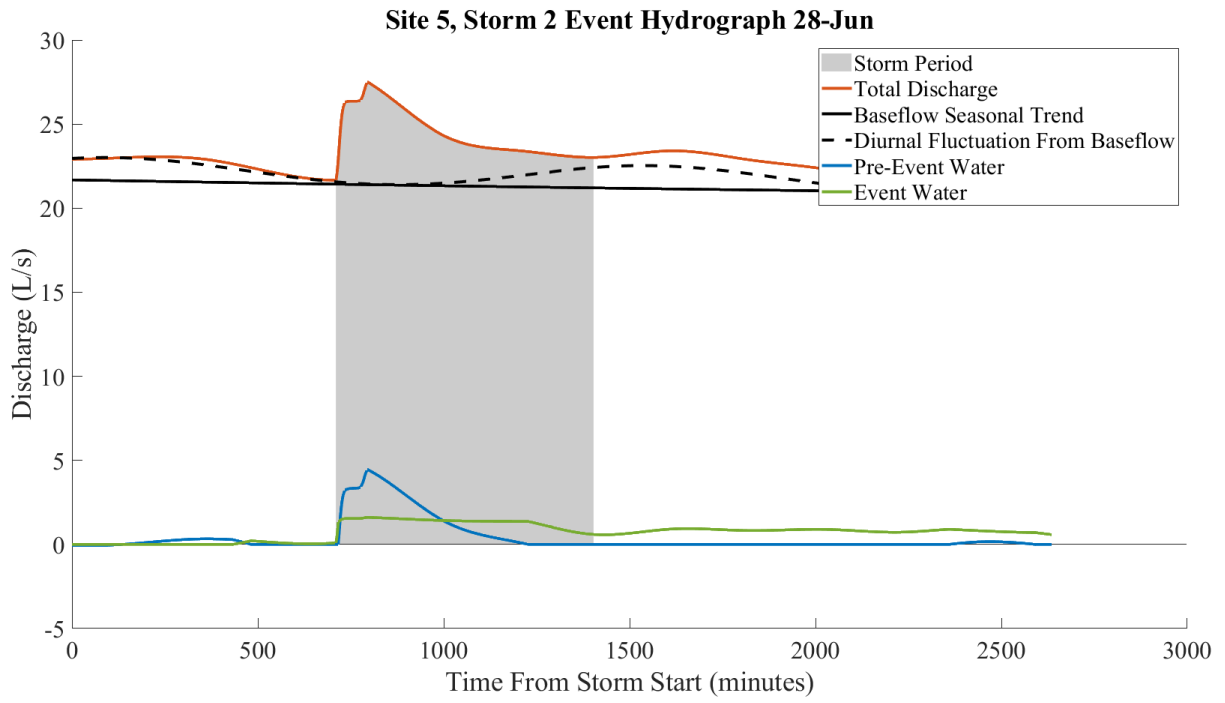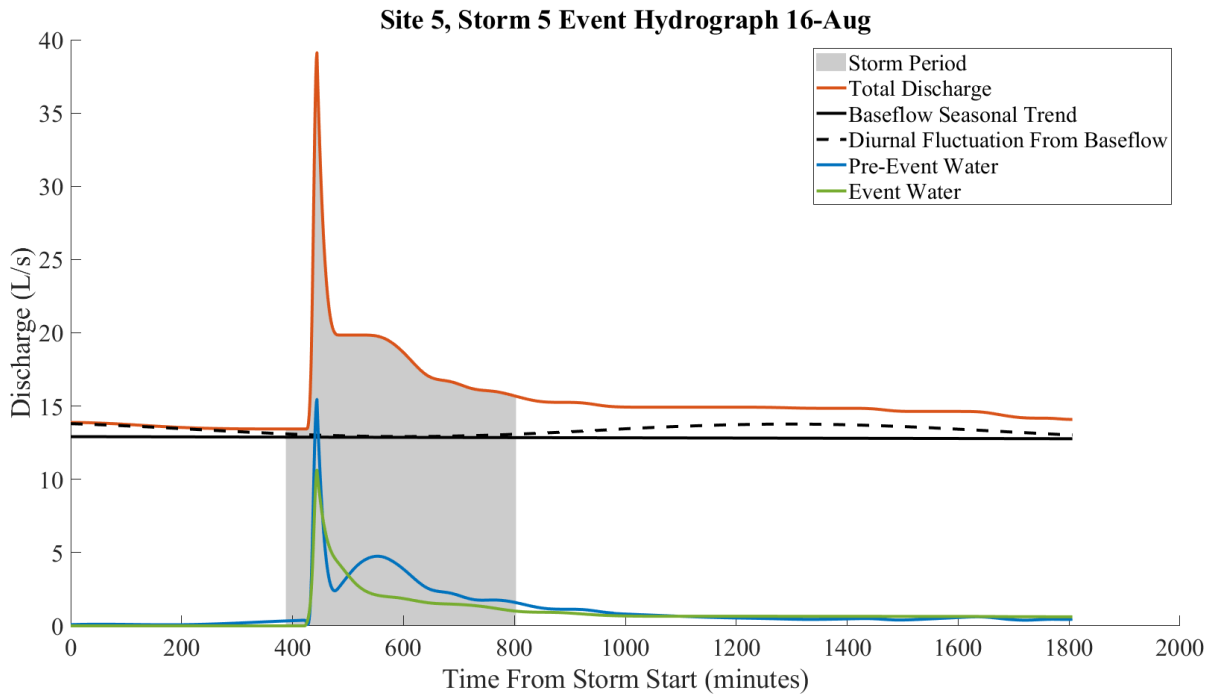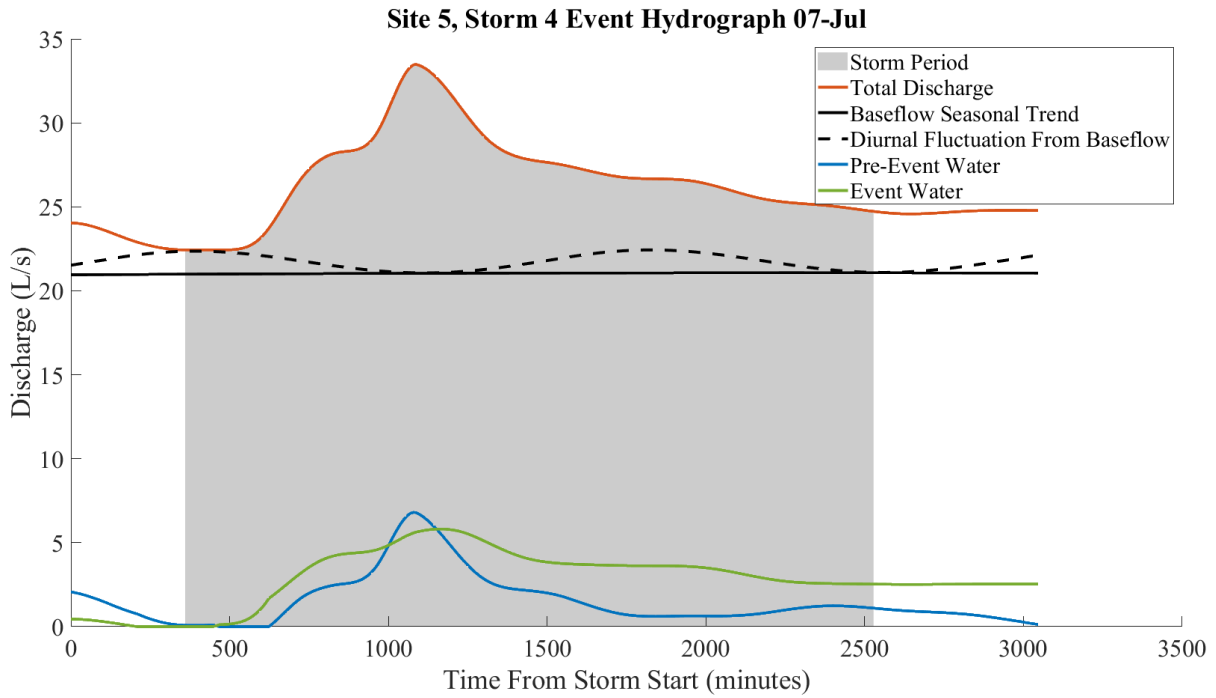
Site 5, Storm 6 Event Hydrograph 18-Aug
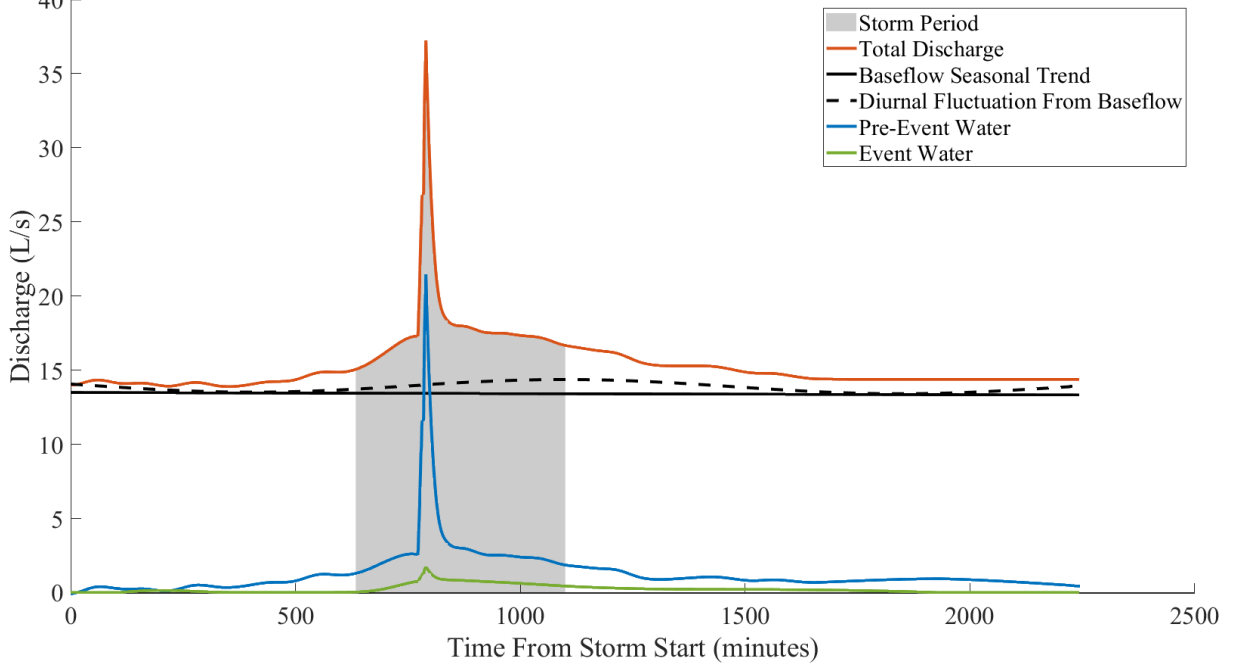
Site 5, Storm 7 Event Hydrograph 06-Oct

Site 8, Storm 1 Event Hydrograph 11-Jun

Site 8, Storm 2 Event Hydrograph 28-Jun

41
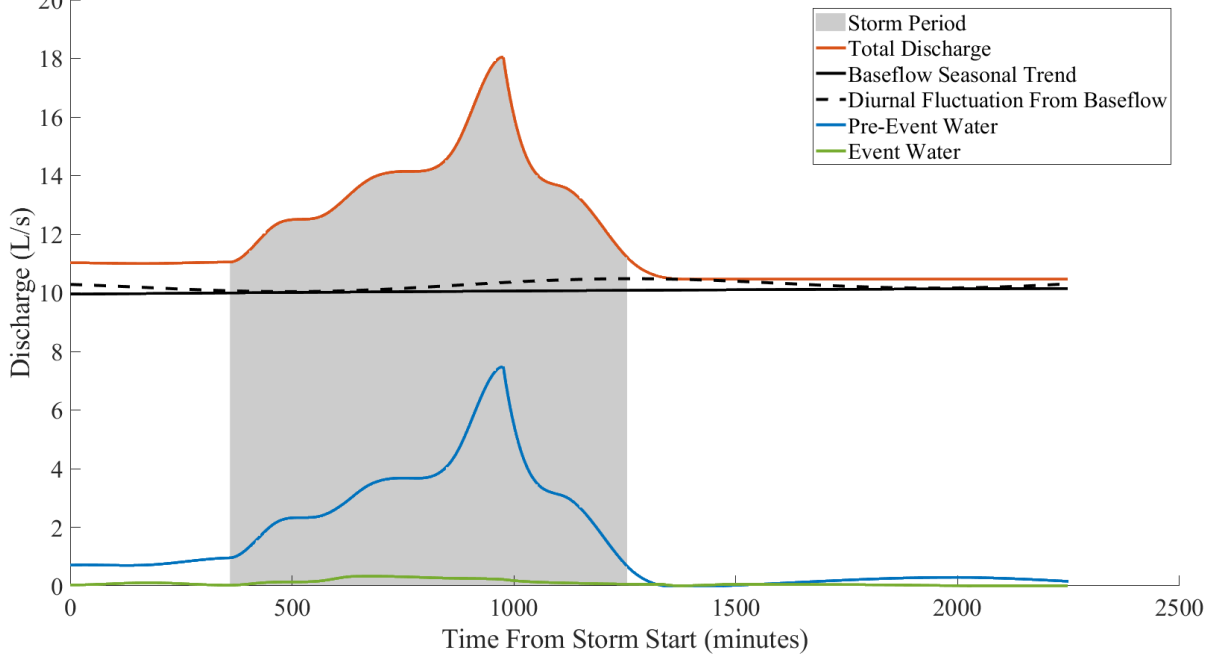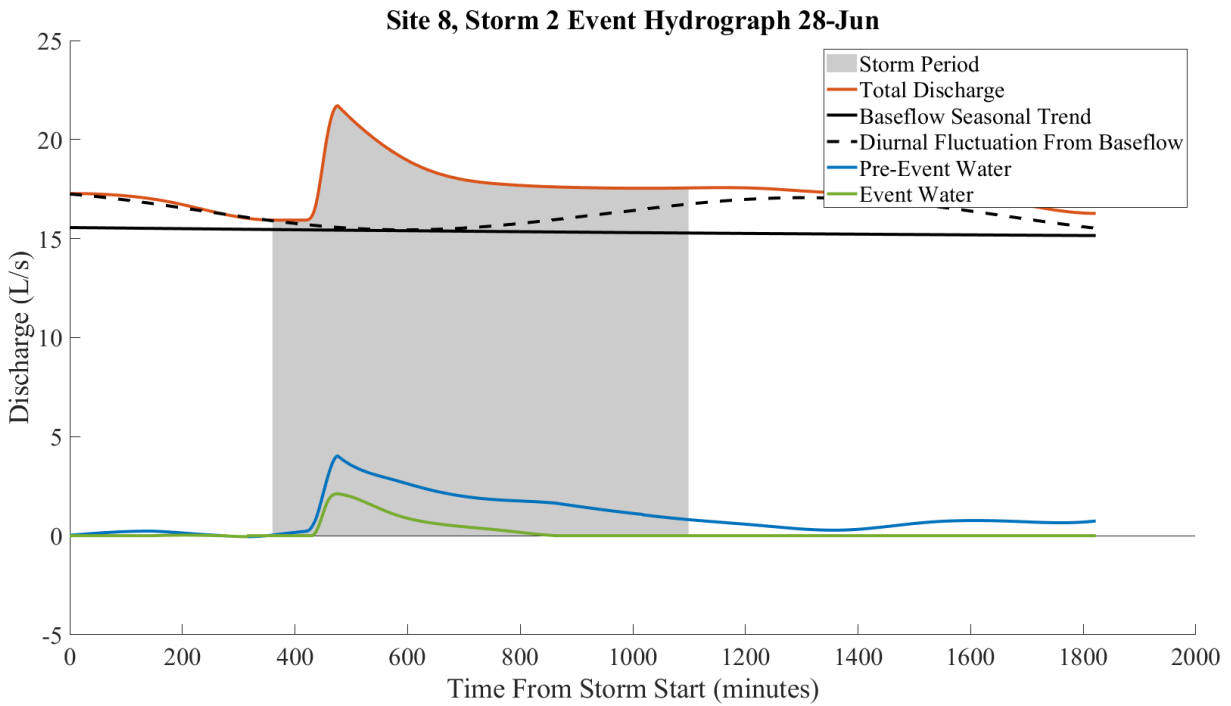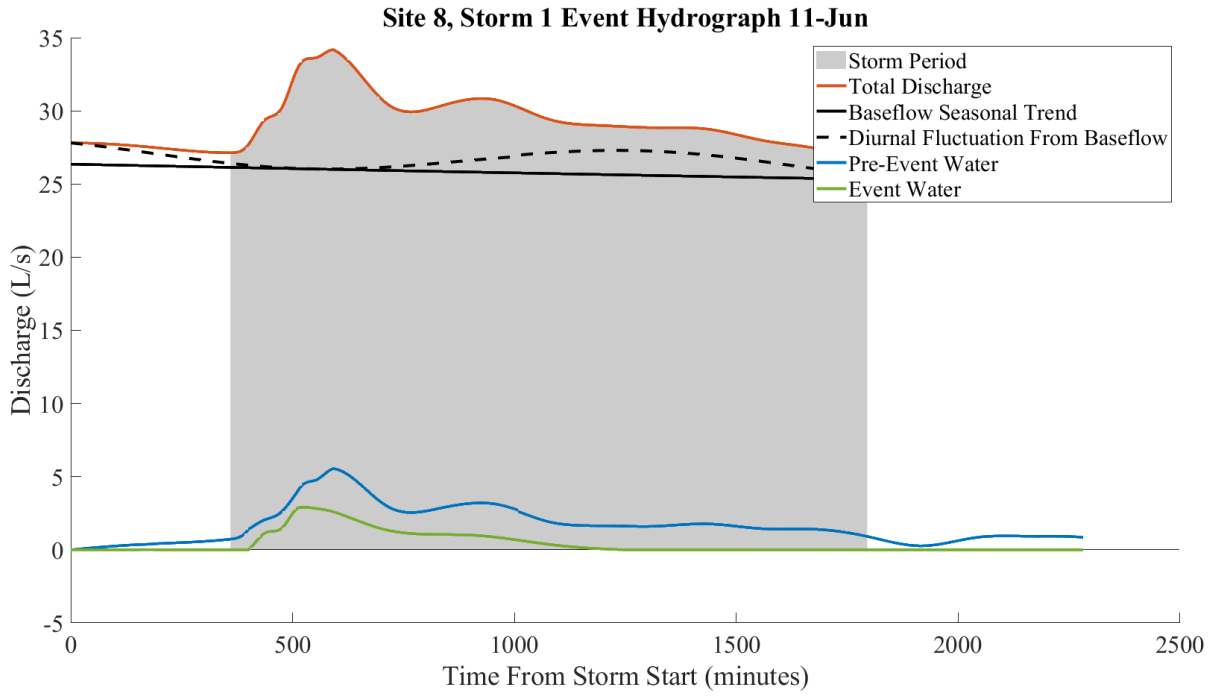
Site 8, Storm 3 Event Hydrograph 01-Jul
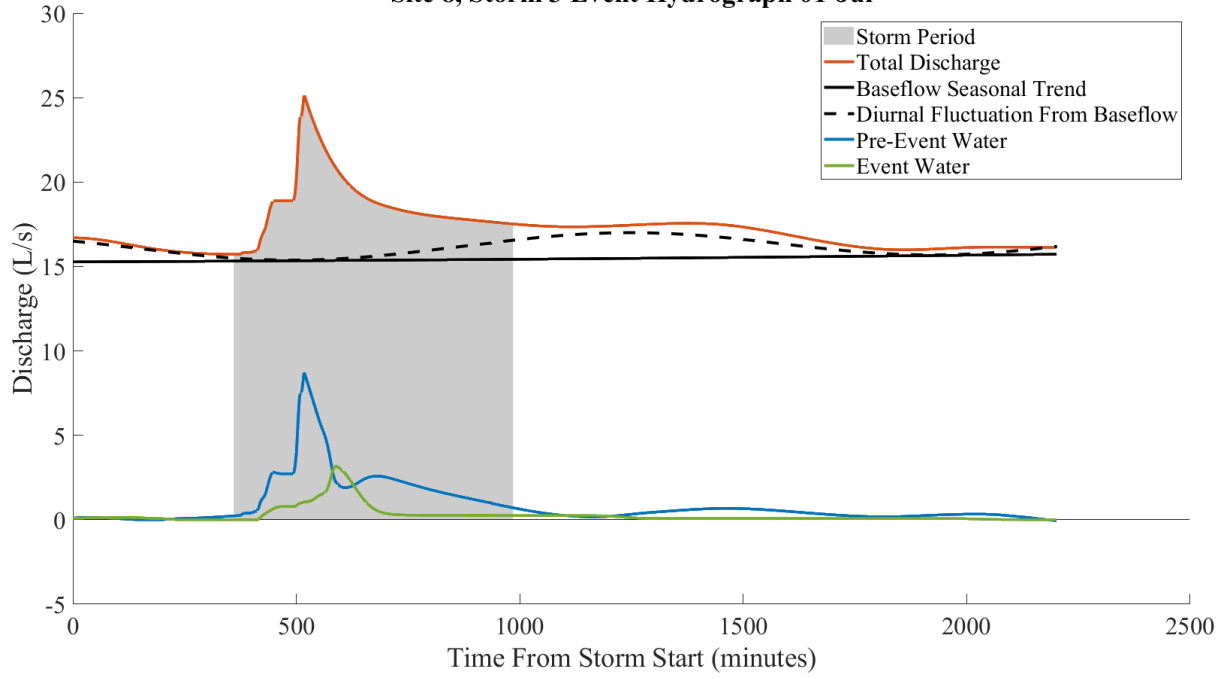
Site 8, Storm 4 Event Hydrograph 08-Jul
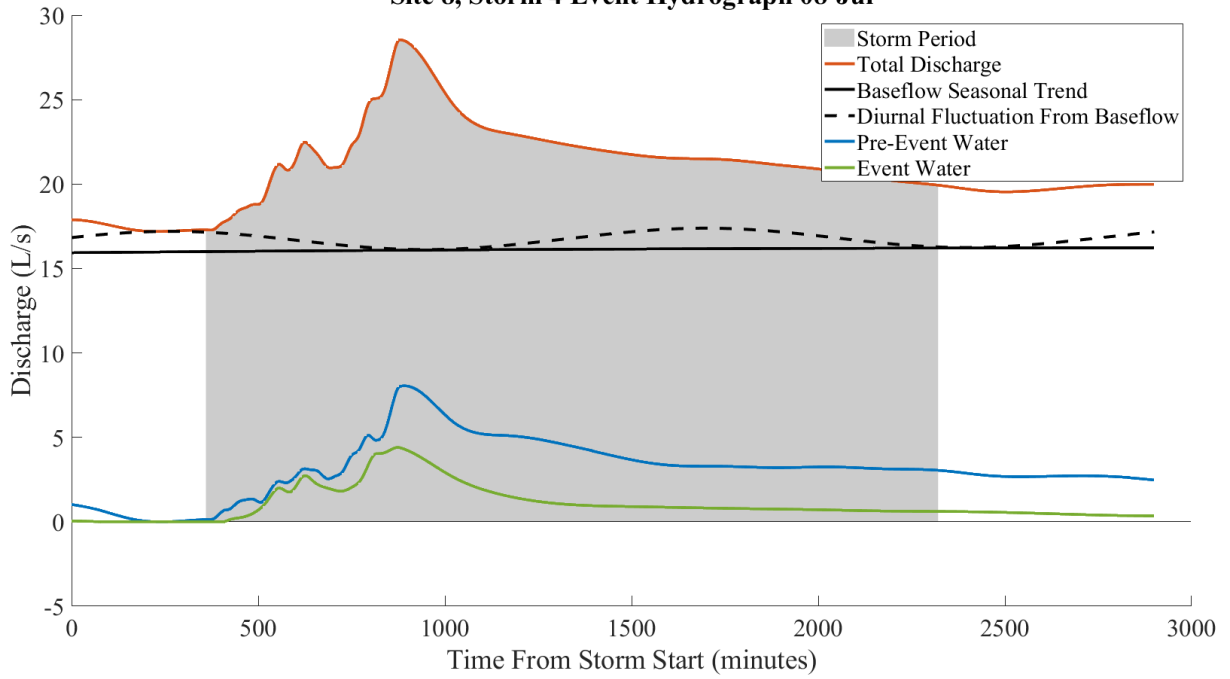
Site 8, Storm 5 Event Hydrograph 16-Aug

Site 8, Storm 6 Event Hydrograph 18-Aug

Site 9, Storm 1 Event Hydrograph 11-Jun

Site 9, Storm 2 Event Hydrograph 28-Jun

Site 9, Storm 3 Event Hydrograph 01-Jul

Site 9, Storm 4 Event Hydrograph 07-Jul

45

Site 9, Storm 5 Event Hydrograph 16-Aug

Site 9, Storm 6 Event Hydrograph 18-Aug

Site 9, Storm 7 Event Hydrograph 06-Oct